UNIVERSITÀ DI SIENA 1240

Dipartimento di Medicina Molecolare e Dello Sviluppo

Dottorato in Medicina Molecolare

XXXVIII° Ciclo

Coordinatore: Prof. Vincenzo Sorrentino

Molecular characterisation of heritable thoracic aortic diseases at the Tuscany referral centre for Marfan syndrome and related disorders

Settore scientifico disciplinare:

PATOLOGIA CLINICA MEDS-02/B (MED/05)

Candidato

Lapo Squillantini

Dipartimento di Medicina Sperimentale e Clinica,

Università di Firenze

Firma digitale del/della candidato/a

LAPO SQUILLANTINI
CN=SQLLPA97D22D612I
31/10/2025 16:06:11
CIE

Supervisore

Dott.ssa Elena Sticchi

Dipartimento di Medicina Sperimentale e Clinica
Università di Firenze

Firmato digitalmente da:
STICCHI ELENA
Università degli Studi di Firenze
Firmato il: 31-10-2025 16:18:38
Seriale certificato: 5949586
Valido dal 19-10-2024 al 19-10-2027

Co-supervisore

Prof.ssa Betti Giusti

Dipartimento di Medicina Sperimentale e Clinica

Università di Firenze

Anno accademico di conseguimento del titolo di Dottore di ricerca

2024/2025

Università degli Studi di Siena
Dottorato in Medicina Molecolare
XXXVIII° Ciclo

Data dell'esame finale

_____

Commissione giudicatrice

_____
_____
_____
_____
_____

Supplenti

_____
_____

Summary

BACKGROUND

A thoracic aortic aneurysm (TAA) is a dilation of the aorta within the chest, which can lead to a life-threatening thoracic aortic dissection (TAD), a tear that allows blood to escape into the aortic wall. TADs are classified by Stanford (Type A involving the ascending aorta, Type B distal to the left subclavian artery) and DeBakey (Types I, II, III based on origin and extent). TAAs are generally classified as syndromic (with additional features outside the aorta, often genetic) or non-syndromic.

- Marfan Syndrome (MFS) is a common genetic connective tissue disorder caused by mutations in the *FBN1* gene. MFS involves skeletal, ocular (ectopia lentis, myopia), and cardiovascular manifestations, primarily aortic root dilatation and dissection. Diagnosis uses the Ghent II criteria, emphasising FBN1 genetic testing and systemic features.

- Loeys-Dietz Syndrome (LDS) is an autosomal dominant connective tissue disorder caused by mutations affecting TGFβ signalling pathway genes (e.g., *TGFBR1*, *TGFBR2*, *SMAD3*, *TGFB2*, *TGFB3*, *SMAD2*, *IPO8*). LDS is characterised by a triad of hypertelorism, bifid uvula/cleft palate, and widespread arterial aneurysms/tortuosity. Aortic dissection in LDS can occur at smaller diameters and younger ages than in MFS.

Non-syndromic TAAs account for about 95% of cases, lacking overt systemic features, and can be familial. Genes like *ACTA2*, *MYH11*, and *PRKG1* are associated with familial non-syndromic forms, affecting smooth muscle contractile proteins. Genetic testing is a valuable tool for early identification and risk assessment, especially for ascending TAAs. Genetic variants significantly influence recommended prophylactic surgical intervention thresholds: MFS patients typically undergo repair at ≤5.0 cm, while LDS patients may require surgery at even smaller aortic diameters. Diagnostic tools include imaging (CT/CTA, MRI/MRA, echocardiography) to assess aortic pathology, clinical evaluation, and some biomarkers. The distinction between syndromic and non-syndromic TAA is increasingly blurred, as variants can lead to a spectrum of phenotypes. This study, conducted at Careggi Hospital, analysed 275 individuals with aortopathy, identifying 37 with pathogenic *FBN1* or TGFβ pathway gene variants.

1. THORACIC AORTIC ANEURYSM AND DISSECTION

The aorta is the largest artery in the body that originates from the heart, curves through an arch in the upper chest, and descends into the abdomen to deliver oxygen and nutrition to distal organs. A thoracic aortic aneurysm (TAA) is a balloon-like bulge or enlargement in the thoracic aorta. The natural history of these aneurysms is that they enlarge over time until a tear forms in the intimal layer of the aortic wall, leading to aortic dissection. While the conventional definition of an arterial aneurysm involves dilation to at least 1.5 times the normal diameter for the abdominal and descending thoracic aorta, this definition is unsuitable for the aortic root and ascending thoracic aorta (1). A thoracic aortic dissection (TAD), also referred to as acute aortic dissection (AAD), is a highly fatal condition that can occur when a tear forms in the intimal layer of the aortic wall. This tear allows blood to penetrate the aortic media, pushing a dissection flap into the middle of the aorta and separating the true lumen from the false lumen. AAD is an emergency condition that can cause sudden death in up to 50% of affected individuals (2). The incidence of AAD has increased over the past 20 years for unknown reasons. Approximately 7% of out-of-hospital sudden deaths are due to AADs (3)

The thoracic aorta is divided into several main segments: the root, ascending thoracic aorta, aortic arch, and descending thoracic aorta. TAAs can occur in any of these segments. Aneurysms of the aortic root and ascending thoracic aorta are typically diagnosed at younger ages compared to those of the descending thoracic aorta, which tend to be degenerative and present later in life. Also, ascending TAAs are more common than descending TAAs (4,5). The Stanford classification distinguishes between two main types of acute aortic dissection (Figure 1):

- Stanford Type A Acute Aortic Dissections, in which the tear occurs above the sinotubular junction, leading to the formation of a false lumen in the aortic wall that may extend to the arch and thoracoabdominal aorta.
- Stanford Type B Acute Aortic Dissections originate in the descending thoracic aorta just distal to the left subclavian artery.

Another commonly used classification is the DeBakey System, which categorises dissections into types I, II, and III, based on the origin of the intimal tear and the extent of the dissection:

- Type I: Dissection tear originates in the ascending aorta and propagates distally to include the aortic arch and typically the descending aorta
- Type II: Dissection tear is confined only to the ascending aorta
- Type III: Dissection tear originates in the descending thoracic aorta and propagates most often distally
    - Type IIIa: Dissection tear is confined only to the descending thoracic aorta
    - Type IIIb: Dissection tear originates in the descending thoracic aorta and extends below the diaphragm

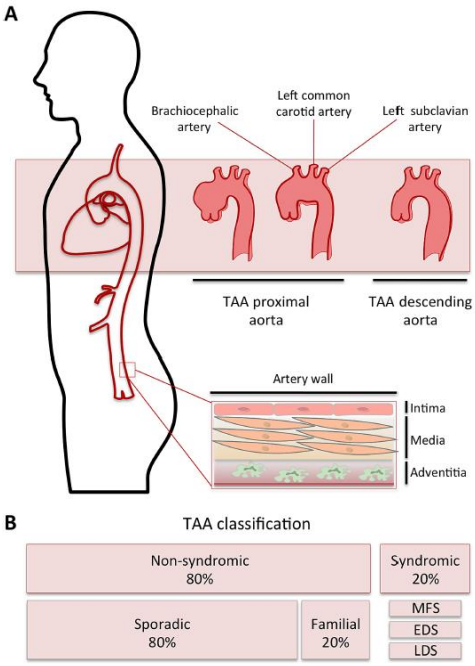

Figure 1. (A) TAA subtypes based on localisation within the aortic tree. (B) TAA classification as syndromic and non-syndromic. Reference [Non-syndromic thoracic aortic aneurysm: cellular and molecular insights, July 2021]

The DeBakey system offers greater anatomic detail, whereas the Stanford system is simpler, essentially distinguishing those dissections that involve the ascending thoracic aorta from those that do not (4). TAA has traditionally been divided based on the presence of extra-aortic clinical manifestations into syndromic TAA or their absence into non-syndromic TAA (Figure 1). Syndromic TAA patients present with systemic features reflecting the presence of diseases involving connective tissue disorders such as Marfan syndrome (MFS), Loeys-Dietz syndrome (LDS), vascular Ehlers-Danlos syndrome (vEDS), and arterial tortuosity syndrome (5). Approximately 20% of families with TAD exhibit an autosomal dominant inheritance pattern, indicating Mendelian inheritance of a pathogenic variant conferring a highly penetrant risk for TAD, the genetic risks for TAD extend from highly rare penetrant variants that trigger disease in almost all individuals carrying the alteration to common and lower penetrant variants more commonly found in the general population that confer a lower risk for disease (6).

Syndromic Thoracic Aortic Aneurysm

Syndromic thoracic aortic aneurysms are characterised by the presence of multisystem features or systemic signs. Subjects usually have a positive family history of aortic aneurysm or dissection, and these conditions are caused by mutations involving extracellular matrix proteins or involved in the transforming growth factor-β pathway. Such patients, including Marfan syndrome (MFS), Loeys-Dietz syndrome (LDS) and Vascular Ehlers-Danlos syndrome (vEDS), are predisposed to developing aneurysms of the aortic root and ascending aorta at an early age, and have a faster rate of aortic growth than do those with sporadic aneurysms. In other cases, such as Bicuspid Aortic Valve (BAV) disease and Turner syndrome, TAAs are a possible manifestation. Those subjects have a higher risk of acute aortic dissection or rupture, resulting in a shorter life

expectancy than those patients whose aneurysms are not genetically mediated (4).

Histologically, LDS and MFS also have similar appearances, namely medial degeneration with little evidence of inflammation, including findings of elastin fragmentation and increased collagen deposition (7). Also, the activation of the TGFβ pathway potentiates inhibitors of tissue proteases such as plasminogen activator inhibitor-1 (PAI-1) and tissue inhibitors of the MMPs (TIMPs). MMPs are essential for normal remodelling and organised matrix deposition, as seen in other tissues such as the skeletal system. Therefore, the result of enhanced activation of cascades involving TGFβ and CTGF is a disorganised tissue remodelling process leading to compromised mechanical integrity. As well as LDS, studies have also shown higher circulating TGFβ in MFS patients compared to healthy controls (8).

Marfan Syndrome and mutations in Fibrillin-1

Marfan Syndrome (MFS, OMIM #154700) is a complicated genetic connective tissue disorder named after Antoine-Bernard Marfan in 1896. It is an autosomal dominant heritable disorder of connective tissues with prominent involvement of skeletal, ocular, cardiovascular and pulmonary organ systems. MFS is the most common genetic disorder of the connective tissue, with an estimated prevalence of 1 in 10,000 (9). In 1991, mutations in the *fibrillin-1* (*FBN1*) gene were identified as the cause of Marfan Syndrome (10). The structure of fibrillin is cysteine-rich, which may be critical for microfibril assembly and may be the means of interaction with TGFβ. They also possess multiple epidermal growth factor (EGF)-like domains that bind calcium (11). Fibrillin contain the known integrin-interacting sequence RGD to support cell adhesion and can be viewed as a physical tether between local cells and their matrix. In the aorta, this contributes to tissue stability. The loss of these vital cell-matrix connections displayed several key features: Elastin degradation, increase MMP activity leading to further matrix degeneration and SMC loss through apoptotic mechanisms

Establish diagnosis of Marfan Syndrome

Early diagnosis of MFS is useful in preventing cardiovascular symptoms and may encourage early treatment of the disease, thereby improving the quality of life of the patients and potentially prolonging their lifespan. Diagnostic criteria involving multiple system manifestation scores and updated diagnostic criteria in 2010 emphasised the importance of fibrillin-1 (*FBN1*) genetic testing. Diagnostic criteria of MFS primarily depend on pathological manifestations of multiple systems and family history. Cardiovascular symptoms of MFS are emphasised in the revised Ghent criteria. In cases without a family history of MFS, patients with aortic root dissection or dilatation (Z-score ≥2) and one of the three MFS-related manifestations (Ectopia Lentis, *FBN1* mutation, the system score ≥7) can be diagnosed with MFS, and MFS diagnosis is also confirmed by the presence of Ectopia Lentis (EL) and *FBN1* mutation associated with aortic disease. Moreover, in cases with a family history of MFS, the presence of EL, or the systemic score (table 1) ≥7 points or aortic root dilatation (Z-score ≥2 in individuals above 20 years old or Z-score ≥3 in individuals below 20 years old) are sufficient for an MFS diagnosis (12). In addition, when clinical manifestations do not meet the diagnostic criterion, gene mutation detection is a suitable means of early

diagnosis (13).

Assessment of the systemic features of MFS, along with the status of the thoracic aorta and *FBN1* genetic testing, are the basis for the Ghent II nosology for the diagnosis of MFS. The systemic features that are present in an individual, excluding thoracic aortic enlargement, result in a composite score up to 20 points (Table 1). In practical terms, the radiologic imaging to identify protrusio acetabulae or dural ectasia is rarely performed when the diagnosis is being considered. If this systemic score is ≥7, it is combined with findings that are common in MFS but rare in the general population, that is, ectopia lentis, thoracic aortic dilatation, and/or a positive family history of MFS, a diagnosis of MFS is achieved. Sequencing of *FBN1* to identify pathogenic variants is not required to make the diagnosis of MFS. However, *FBN1* sequencing ensures that the MFS systemic features and thoracic aortic disease are not the result of pathogenic variants in another gene, for example, *TGFBR2* or *TGFBR1* (14).

Table 1. Scoring of systemic features. Reference [The revised Ghent nosology for the Marfan syndrome, July 2010]

Features	YES	NO
Wrist AND thumb sign	3	0
Wrist OR thumb sign	1	0
Pectus carinatum deformity	2	0
pectus excavatum or chest asymmetry	1	0
Hindfoot deformity	2	0
Plain flat foot	1	0
Pneumothorax	2	0
Dural ectasia	2	0
Protrusio acetabulae	2	0
Reduced US/LS and increased armspan/height	1	0
Scoliosis or thoracolumbar kyphosis	1	0
Reduced elbow extension	1	0
3/5 facial features	1	0
Skin striae	1	0
Myopia	1	0
Mitral valve prolapse	1	0

There are some related disorders of Marfan disease in which patients can be found to have a *FBN1* variant. MASS Phenotype is a connective tissue disorder that is similar to Marfan syndrome in that people with the condition have the similar Mitral valve, Aorta, Skin, and Skeletal features. People with the MASS phenotype do not have lens dislocation and do not show progressive and dangerous aortic root enlargement, hallmark features of Marfan syndrome. Ectopia Lentis Syndrome is an inherited connective tissue condition that shares some of the features of Marfan syndrome, particularly lens dislocation of the eye, which can cause serious vision problems. People with ectopia lentis syndrome do not have the heart and blood vessels problems associated with Marfan syndrome (12,15).

In the majority of MFS patients, thoracic aortic disease begins as an asymptomatic enlargement of the aortic root, which progressively enlarges over time to form an aneurysm (a weakening of the artery wall leading to a bulge or distention). Medications can slow the rate of enlargement, but do not prevent it. The aortic aneurysm becomes unstable as it enlarges and ultimately may lead to an acute ascending aortic dissection. Currently, proper diagnosis and management of thoracic aortic aneurysms in individuals with MFS can prevent most acute type A aortic dissections, and since the 1970s, patients with MFS have a life expectancy that approaches that of the general population (16). The most frequent aortic event associated with MFS is the dilatation of the aortic root, the aortic segment closest to the heart. Dilatation of the aortic root is usually symmetrical and limited to the aortic root, at least at the beginning of disease progression. Aortic root dilatation has a diagnostic value, but the normal aortic root diameter has to be adjusted using nomograms that include age, sex, height and weight. In addition to diagnosis, the degree of aortic root enlargement also carries crucial prognostic information, specifically the risk of aortic dissection (17). Dilatation of the tubular ascending aorta can be observed in patients with MFS and is almost always associated with substantial dilatation of the aortic root. The additional dilatation of the tubular aorta is considered to indicate a higher risk for aortic dissection than dilatation of the aortic root alone (18). The largest diameter of the ascending aorta, regardless of whether it is in the root or the tubular ascending aorta, is used to determine the timing of prophylactic repair of the aneurysm to prevent an acute type A aortic dissection. In most cases, the dissection can propagate further up to the distal parts of the ascending aorta and continues down the descending aorta. Alternatively, the blood can dissect proximally and rupture into the pericardial sac, and the majority of people who die suddenly owing to dissections die of pericardial tamponade (19). Individuals with MFS are also at risk for aortic dissections originating at a different aortic location, just distal to the orgin of the left subclavian artery (a branch of aortic arch going to the brain) and progressing down the descending aorta, termed type B dissections. These dissections less commonly cause sudden death and occur with little to no enlargement at the site of origin of the dissection. Complications requiring surgery can occur with type B dissection and include malperfusion of spinal arteries leading to paresis and paraplegia, malperfusion of visceral arteries leading to abdominal pain, and aortic rupture. In individuals with MFS, initial presentation with a type B dissection is less frequent than presentation for prophylactic aneurysm repair or type A dissection (20).

MFS is also associated with complications involving the heart. Stretching of the aortic valve annulus due to aortic root enlargement may give rise to leaflet malcoaptation in which the leaflets fail to join together at the closure of the valve, and aortic valve regurgitation. This presentation is often combined with aortic valve cusp prolapse and valve cusp commissural fenestrations (ovoid apertures). A study in paediatric patients with MFS (< 18 years of age), moderate to severe aortic valve regurgitation was found to be an independent predictor of aortic root growth and cardiovascular events (for example, death, aortic dissection and cardiac valve or aortic root surgery) (21). Mitral valve prolapse (MVP) and mitral valve regurgitation (MVR) are established complications in

patients with MFS. The prevalence of MVP in adults with MFS is estimated between 40% and 68% (compared with 1–2% in the general population). A population-based study found that patients with MFS have an increased risk of 28% for mitral valve-related clinical events (endocarditis, surgery, and heart failure), compared with 13% in idiopathic MVP. The age at the time of the event was also significantly lower in individuals with MFS than in individuals with MVP not associated with MFS. Severe mitral regurgitation due to degenerative mitral valve disease may be successfully repaired in MFS, but it is often a more complex procedure than the same procedure performed in the general population. More recently, mitral annulus disjunction (MAD) was found to be highly prevalent in patients with MFS. MAD was a marker of severe disease, including aortic events at younger ages and mitral valve disease requiring repair. Thus, detection of MAD may infer close clinical follow-up. Pulmonary artery dilatation occurs in children and in adults with MFS and is correlated with aortic root dilatation, previous aortic root surgery, reduced left ventricular ejection fraction and increased pulmonary artery systolic pressure. Clinical complications of pulmonary root dilatation are rare and may occur only with associated increased pulmonary artery pressure. Heart failure is the cause of death in 5–30% of patients with MFS. Underlying causes are severe valvular dysfunction and an intrinsic myocardial dysfunction. The reported prevalence of 'Marfan cardiomyopathy' ranges from 3% to 68% across different series. Mild cardiomyopathy usually does not evolve with time but can lead to an unfavourable course in the event of an additional hemodynamic trigger, such as valve dysfunction and / or aortic root replacement. Several studies have reported end-stage heart failure necessitating heart transplantation in patients with MFS (14). Children and adults with MFS have a predisposition for supraventricular as well as ventricular arrhythmias (that is, irregular heartbeat), which are not always related to valvular abnormalities. several studies report life-threatening ventricular arrhythmias in 7–9% of individuals in MFS cohorts, along with sudden cardiac arrest in up to 4% of individuals, which is most likely due to arrhythmia. A possible association with underlying intrinsic myocardial dysfunction, as described above, is supported by the finding that serum NT-proBNP levels (which increase as a result to damage to the myocardium) are the strongest independent predictor of arrhythmogenic events in patients with MFS (22,23).

MFS is associated with substantial musculoskeletal abnormalities due to three pathophysiological processes. First, the growth of tubular bones is exaggerated, which results in elongation of the digits (arachnodactyly), legs leading to disproportionate tall stature (dolichostenomelia) and ribs (leading to pectus excavatum or carinatum). Second, ligamentous laxity leads to joint hypermobility, especially of the digits, shoulders, knees, and ankles, and progressive vertebral column deformity (scoliosis). Third, progressive deformity of some areas leads to depressed hip joints (protrusion acetabulae) and thinning and widening of the lumbar vertebrae and neural foraminae (dural ectasia). Additionally, most patients develop degenerative arthritis earlier than expected (24).

The ocular manifestations in patients with MFS vary by mutation and resulting severity of the disease. Patients with typical features of MFS develop lenticular and/or axial myopia prior to ten years of age and should be referred to an ophthalmologist for assessment of their nearsightedness. If the lens is

dislocated in one or both eyes, the diagnosis of MFS should be suspected and confirmed based on the Ghent II criteria. In the absence of lens dislocation, enlarged corneal diameter, corneal astigmatism, miosis (excessive constriction of the pupil) and hypoplasia of the iris may suggest a diagnosis of MFS. About 60% of MFS patients will develop lens dislocation in their lifetime, with the majority of patients being diagnosed in their teens, when the growth of the ocular globe is complete, but lens dislocation may occur late into their seventies. Both corneal and lenticular astigmatism are common and severe. Strabismus secondary to amblyopia (lazy eye) may arise in the first decade of life, because the lens dislocation is typically asymmetric leading to preference of the less severely affected eye. The resulting amblyopia in the fellow eye is rarely deep-seated and can be reversed with careful refraction assessment and glasses or contact lenses. Presenile cataracts are a common complication in patients with MFS. Open-angle glaucoma and retinal detachments are the complications that lead to vision loss in patients with MFS. In patients with the most severe form of MFS, neonatal MFS, the globe is typically enlarged at birth with an increased corneal diameter. In rare patients, open-angle glaucoma is observed in the first few years of life. The pupil will be miotic preventing the microspheric lens from prolapsing into the anterior chamber, and pupillary block is rare. Very high myopia up to thirty diopters may be observed; it is usually composed of both lenticular and axial myopia (14).

Variants on *FBN1* and correlation with clinical manifestations

The majority of *FBN1* mutations in Marfans are point mutations, though frameshift, nonsense and splice-site mutations also exist, in addition to whole-exon or even whole-gene deletions (25,26). This strongly suggests the loss of function of the FBN1 protein as the relevant mechanism. Substitutions of cysteine residues that alter the disulfide bonds within the EGF or cysteine-binding modules are the most frequent mutations. These structural alterations impair the organisation of the fibrillin into microfibril bundles. In a mouse model of MFS, the *FBN1* knockout, the appearance of the aorta displays elastin degradation and disorganisation along with considerable loss of *FBN1* (27). *FBN1* knockout mice die within one year of birth due to aortic dissection and rupture: aneurysms initiate within 2 weeks of birth and continue to enlarge with time (28). In addition, *FBN1* mutations substantially impact fibrillin's ability to bind and sequester TGFβ, leading to increased free TGFβ and excessive signalling of this pathway (29). Several trials have therefore attempted to use inhibitors of TGFβ signalling, namely Losartan, to halt TAA progression in MFS, particularly in children, though its efficacy in comparison to beta-blockade was not established (30,31).

Aortic development in patients with MFS presents sexual dimorphism. Aortic aneurysms in patients with MFS are more severe in males compared with females (32). The mutational heterogeneity of *FBN1* may cause age-related penetrance and diversification in clinical manifestations of MFS (33). Different mutations cause the sequestering of mutant protein in the endoplasmic reticulum then exerting haploinsufficiency (HI) efforts or promoting secretion of mutant protein in the ECM and exerting dominant-negative (DN) efforts. Pathogenic mechanisms and clinical manifestations of MFS may be related to the positional effects of mutations in *FBN1*, and dominance of the mutant alleles.

In the DN model, *FBN1* mutant alleles interfere with the function of the protein encoded by the wild-type allele, thereby causing the appearance of MFS (34). And the HI model refers to the failure of microfibrillar assembly ascribed to HI of normal FBN1 rather than the mutant protein. About one-third mutations of *FBN1* result in HI effects including nonsense, splicing or out-of-frame mutations, and other two-third mutations lead to DN effects including missense, splicing and in-frame mutations (35). Some correlations of genotype/phenotype have been discussed. The widely accepted correlation is that large proportions of MFS children carry mutations located in exons 24-32 and in-frame mutations of *FBN1*, particularly in neonatal patients (36). And patients with mutations in exons 43-65 show the same high frequency of major cardiovascular phenotype compared with exons 24-32 (37). Patients with mutations in exon 1-21 present with a high incidence of EL, and patients with mutations in exons 23-32 are more likely to develop aortic root dilatation (38). The more severe musculoskeletal and skin phenotype are observed in patients with an *FBN1* premature termination codon when compared with those in an in-frame mutation of *FBN1*. Patients with a missense mutation of *FBN1* involving a cysteine residue have a high risk of EL, and a mutation eliminating a cysteine shows a higher presence of aortic dilation and Mitral Valve Prolapse (MVP) than those with creating a cysteine (25).

Loeys-Dietz Syndrome and Mutations in TGFβ Signalling-Related Genes

Loeys-Dietz syndrome (LDS, OMIM #609192, #610168, #613795, #614816, #615582, #619656) is an autosomal dominant connective tissue disorder; LDS is typically characterised by a combination of vascular, skeletal, craniofacial, cutaneous, and ocular abnormalities (39). LDS is strictly clinically characterised by the triad of hypertelorism, bifid uvula/cleft palate, tortuosity and aortic/arterial aneurysms. Vascular problems are the most severe concern in LDS, as the disorder causes widespread aneurysms and tortuosity of arteries throughout the body. These aneurysms are prone to dissection and rupture at younger ages and smaller diameters than in other syndromic conditions (like Marfan syndrome); this issue is significantly associated with this condition when pathogenetic mutations involve specific genetic loci [i.e. genes encoding transforming growth factor β (TGFB) receptor 1 (*TGFBR1*) and 2 (*TGFBR2*)] (40). LDS is caused by mutations that affect different genes coding transforming growth factor β signalling pathway members and, according to the genes involved, different types have been described (Table 2). LDS type 1 (LDS1) and type 2 (LDS2) are linked to mutations in *TGFBR1* and *TGFBR2* genes, respectively; with arterial tortuosity, bifid uvula, and hypertelorism as phenotypic manifestations observed in these subjects (40,41). LDS type 3 (LDS3) represents a further LDS type in which mutations in the gene (*SMAD3*) coding the *mothers against decapentaplegic homolog (SMAD) 3* (a component of SMAD proteins family involved in the transforming growth factor β signalling pathway, so allowing signals transmission from the cell surface to the nucleus, regulating gene activity and cell proliferation) have been recognised, exhibiting hereditary thoracic aortic disease (HTAD) and significant osteoarthritis features. Moreover, *SMAD3* variants have been also observed in subjects showing aneurysms affecting the abdominal aorta and various other arteries, including the branch vessels of the aorta and intracranial arteries (42–44). Furthermore, LDS types 4 (LDS4) and 5 (LDS5) are related to mutations in the genes encoding *TGFB2* and *TGFB3* ligands,

respectively (45,46). The various Loeys-Dietz syndrome (LDS) types exemplify the degree of clinical severity according to the different clinical manifestations, with type 1 representing the most severe form and type 5 the less severe (41,47). Moreover, mutations in the *SMAD2* gene have also been recognised as linked to the phenotypic spectrum of Loeys-Dietz syndrome (LDS); however, its classification within the LDS types remains to be established for some authors while others recognise a further LDS form (type 6) (48–50). Recently, it has been reported that bi-allelic loss-of-function variants in *IPO8* cause a syndromic form of thoracic aortic aneurysm (TAA) with a clinical overlap with Loeys-Dietz and Shprintzen-Goldberg syndromes (51). As a result, mutations in genes that encode various components of the TGFβ signalling pathway disrupt the normal development of the extracellular matrix, leading to multisystemic abnormalities (42).

Table 2. Loeys-Dietz Syndrome (LDS): Associated Genes and Subtypes. Reference [Loeys-Dietz Syndrome, Updated 2024 Sep 12]

Gene	Subtype of LDS	Comment
TGFBR1	LDS1	Most severe phenotype; phenotype for TGFBR1- & TGFBR2-related LDS is similar in severity.
TGFBR2	LDS2	
SMAD3	LDS3	Severity of aortic disease in SMAD3-related LDS is similar to TGFBR1- or TGFBR2-related LDS; strong predisposition for osteoarthritis
IPO8	LDS7	Very severe aneurysms at young age; no dissections described
TGFB2	LDS4	Systemic findings possibly less severe & more like Marfan syndrome
SMAD2	LDS6	Variable cardiovascular phenotype, incl congenital heart disease
TGFB3	LDS5	Mildest form of LDS

Patients with LDS show many phenotypic features that overlap with those of MFS such as scoliosis, arachnodactyly, pectus deformity and importantly aortic aneurysm centered at the sinuses of Valsalva. The natural history of LDS is characterized by aggressive arterial aneurysm and a high incidence of pregnancy-related complications, including uterine rupture and death. Aortic dissection has been observed as early as early childhood and at aortic dimensions that do not confer the risk of dissection or rupture in other aortopathies. Compared to MFS, the arterial involvement is more diffuse with arterial tortuosity present in most individuals, affecting the head and neck vessels (52). TGFβ signalling is enhanced in LDS, which is thus detected by elevated connective tissue growth factor (CTGF) expression and nuclear *SMAD2* localisation, the up-regulation of CTGF could in-turn propagate excessive TGFβ

signalling via attenuation of the inhibitor *SMAD7*, a key component of the TGFβ feedback loop (40,41). Evidence suggests that the signalling cascade distal to the TGFβ receptor is key to its pathogenesis. LDS-causing mutations in the *TGFBR1* and *TGFBR2* genes, mostly missense changes, cluster around the receptor kinase domains, which are regions of the receptor protein that potentiate canonical TGFβ signalling. Interestingly, the loss of function mutations in *TGFBR1* cause Ferguson- Smith Disease and not LDS, which have entirely different clinical manifestations (Ferguson-Smith Disease presents with multiple spontaneous epitheliomas and not the features of LDS, including TAA and TAAD) (53). *TGFBR1* and *TGFBR2* are activated in tandem leading to phosphorylation of receptor proteins such as *SMAD2* and *SMAD3*, which translocate to the nucleus as transcriptional modulators. Patients with the loss of function mutations in *SMAD3* were found to show the complete phenotypic picture of LDS (42). Despite this, evidence suggests that the overactivation of TGFβ signalling is the pathogenic process leading to aneurysm formation and LDS. Tissue obtained from patients with *SMAD3* or *TGFB2* mutations obtained at the time of aortic surgery show the characteristic signature of increased rather than decreased TGFβ signalling (increased phosphorylation of SMAD proteins and increased expression of TGFβ ligands) (46).

Establish diagnosis of Loeys-Dietz Syndrome

The clinical diagnosis of LDS can be established in a proband with suggestive findings. However, no consensus clinical diagnostic criteria are published. The molecular diagnosis of LDS can be established in a proband who has a heterozygous pathogenic (or likely pathogenic) variant in *SMAD2*, *SMAD3*, *TGFB2*, *TGFB3*, *TGFBR1*, or *TGFBR2* or biallelic pathogenic (or likely pathogenic) variants in *IPO8* AND any of the following

- Aortic root enlargement (defined as an aortic root z score ≥2 standard deviations above the mean) or type A dissection
- Other characteristic clinical features of LDS: craniofacial, skeletal, cutaneous, and/or vascular manifestations (especially arterial tortuosity, prominently including the head and neck vessels, and aneurysms or dissections involving medium-to-large muscular arteries throughout the arterial tree)
- Family history of established diagnosis of LDS (54).

Clinical Features of Loeys-Dietz Syndrome

Loeys-Dietz syndrome (LDS) represents a wide phenotypic spectrum in which affected individuals may have various combinations of clinical features ranging from a severe syndromic presentation with significant extravascular systemic findings in young children to predominantly thoracic aortic aneurysm/dissection occurring in adults (Figure 2).

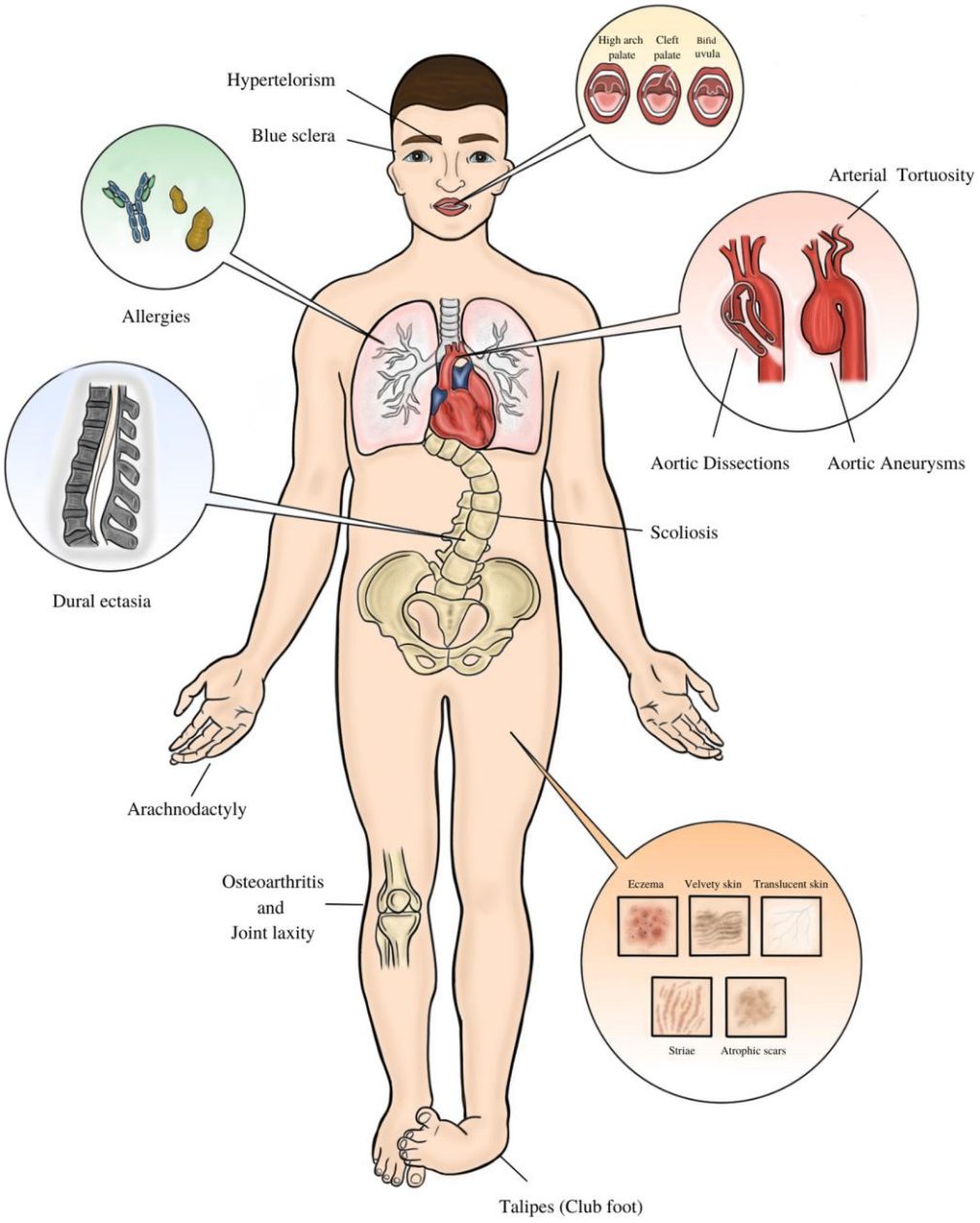

Figure 2. Spectrum of common features and complications of Loeys Dietz. Reference [Clinical features and complications of Loeys-Dietz syndrome: A systematic review, September 2022]

Clinical variability is also observed among individuals in the same family who have the same pathogenic variant. The major sources of morbidity and early mortality in LDS are dilatation of the aorta at the level of the sinuses of Valsalva,

a predisposition for aortic dissection and rupture, mitral valve prolapse (MVP) with or without regurgitation, and enlargement of the proximal pulmonary artery. Arterial aneurysms have been observed in almost all side branches of the aorta including (but not limited to) the subclavian, renal, superior mesenteric, hepatic, and coronary arteries. Aortic dissection has been observed in early childhood (age ≥6 months) and/or at aortic dimensions that do not confer risk of dissection in other connective tissue disorders such as Marfan syndrome. Morover, Arterial tortuosity can be generalized but most commonly involves the head and neck vessels. MVP with mitral regurgitation has been observed in individuals with LDS, although less frequently than in Marfan syndrome. Other recurrent cardiovascular findings include patent ductus arteriosus, atrial septal defects, and bicuspid aortic valve. Although all these findings are common in individuals who do not have LDS, the incidence in LDS exceeds by at least five times that seen in the general population.

Skeletal overgrowth in LDS is less pronounced than in Marfan syndrome and usually affects the digits (arachnodactyly) more prominently than the long bones. Dolichostenomelia (leading to an increase in the arm span-to-height ratio and a decrease in the upper-to-lower segment ratio) is less common in LDS than in Marfan syndrome. Overgrowth of the ribs can push the sternum in (pectus excavatum) or out (pectus carinatum). Joint hypermobility is common and can include congenital hip dislocation and recurrent joint subluxations. Paradoxically, some individuals can show reduced joint mobility, especially of the hands (camptodactyly) and feet (clubfeet). Spine anomalies, including congenital malformations of the cervical vertebrae and cervical spine instability, are common, especially in individuals with more severe craniofacial features. In their most severe presentation, craniofacial anomalies in individuals with LDS are characterized by hypertelorism and craniosynostosis. Craniosynostosis most commonly involves premature fusion of the sagittal suture (resulting in dolichocephaly). Coronal suture synostosis (resulting in brachycephaly) and metopic suture synostosis (resulting in trigonocephaly) have also been described. Bifid uvula is considered the mildest expression of a cleft palate and sometimes the uvula has an unusual broad appearance with or without a midline raphe. Other craniofacial characteristics may include malar flattening and retrognathia. Myopia is less frequent and less severe than that seen in Marfan syndrome. Significant refractive errors can lead to amblyopia. Other common ocular features include strabismus and blue sclerae. Retinal detachment has been reported rarely. Ectopia lentis is not observed except in exceedingly rare case reports of unclear significance.

As in other connective tissue disorders, pneumothorax occurs at increased frequency. Precise incidence estimates have not been determined. Life-threatening manifestations include spontaneous rupture of the spleen and bowel, and uterine rupture during pregnancy. Individuals with LDS are predisposed to developing allergic disease including asthma, food allergy, eczema, allergic rhinitis, and eosinophilic gastrointestinal disease. Some affected individuals have exhibited elevated immunoglobulin E levels, eosinophil counts, and T helper 2 (TH2) cytokines in plasma (54).

Variants on the TGFβ-Pathway and correlation with clinical manifestations

Nearly all mutated patients in a study about 24 families with variants on the *TGFBR1* and *TGFBR2* genes displayed ascending/aortic root aneurysm, early aortic dissection is more rarely reported together with arterial tortuosity. Moreover, Valve abnormalities, in particular mitral valve prolapse and insufficiency, affected nearly half of the patients. Craniofacial features may be considered to be characteristics of LDS1 and LDS2 including dolichocephaly, hypertelorism, malar hypoplasia and highly arched palate, while abnormal palate/bifid uvula was not as frequently found as described in the literature. Recurrent skeletal anomalies included scoliosis, pes planus, long slender fingers, marfanoid habitus, and pectus deformity (55).

Among the LDS-associated genes, *SMAD3* encodes a protein consisting of two globular domains (MH1 and MH2) connected by a linker region. The N-terminal MH1 domain is responsible for DNA binding, while the MH2 domain mediates protein-protein interaction with numerous regulator and effector proteins (56). Data concerning correlations between the type of variants and the patient's phenotype have been reported. Hostetler et al. (57) have shown that the median age of the first aortic event was significantly lower in patients with missense variants in MH2 rather than haploinsufficiency variants (HI). Conversely, in a similar study in a smaller cohort, no significant differences in the aortic phenotype were appreciated (58). Furthermore, a functional study (59) performed on patient-derived fibroblasts and vascular smooth muscle cells (VSMCs) has shown a reduced differentiation potential for fibroblasts from LDS patients with dominant negative *SMAD3* variants compared to those obtained from HI *SMAD3* variant fibroblasts, supporting previous observations from Hostetler et al. (57). Moreover, a retrospective study from de Demolder et al. showed that in patients with HTAD, arrhythmia, and impaired myocardial function were found in patients harbouring Likely Pathogenic/Pathogenic variants in the *FBN1* gene and the TGF-β signalling genes (60). Conversely, other studies reported severe non-aortic cardiovascular phenotypes and suggested a heightened risk of ventricular arrhythmias and sudden cardiac death, which may or may not be associated with pre-existing myocardial dysfunction. These unusual presentations warrant awareness of myocardial disease in patients with *SMAD3* variants and demand further investigation (42,58,61–64). Limited numbers are available in the literature about genotype-phenotype correlation for the other genes associated with LDS (*TGFB2*, *TGFB3* and *SMAD2*).

Non-Syndromic Thoracic Aortic Aneurysm

Non-syndromic TAA is a form of heritable thoracic aortic disease (HTAD), It is characterized by the absence of extra-aortic clinical manifestations or systemic features, Non-syndromic TAAs account for the majority of TAA cases (about 95%) (65), they are further classified as sporadic or familial, in the case of at least one of the first-degree family members being affected (66). According to the ESC (European Society of Cardiology) guidelines, TAA presentation has an impact on management, measures of intervention, and therapeutic strategies, as aortic growth speed and progression vary between syndromic and non-syndromic cases and also between sporadic and familial ones (67). Thus, early identification of asymptomatic patients is crucial to allow timely monitoring and management strategies that could potentially prevent the progression of TAA and TAD, This is especially important in non-syndromic cases in which the lack of distinct clinical manifestations (involving musculoskeletal or ocular signs) may delay detection

(65).

Aortic samples from sporadic ascending TAAs showed that decreased collagens type I and III and increased collagens α1(XI) and V were linearly correlated with the size of the aneurysm (68). In this context, cyclic mechanical stress constantly increases the synthesis, secretion, and assembly of tropocollagen into fibers via intensified Ang-II activity and TGFβ/Smad signaling (69). In human non-syndromic TAA samples, an increase in Smad2 activation was associated with disruption of elastic lamellae (70). Furthermore, an enhancement of TGF-β signaling and Smad2 activation was detected in the aortic wall of ascending TAA patients, whatever the etiology, with the resulting increase in TGF-β1 and phosphorylated Smad2 protein levels (71). This is in line with the described dysregulation of TGF-β signaling in syndromic and familial non-syndromic TAA.

Diagnostic tools used in the management of thoracic aortic aneurysms (TAA)

the diagnostic tools used in the management of thoracic aortic aneurysms (TAA) encompass several categories, primarily focusing on imaging, genetic evaluation, and laboratory tests, complemented by clinical assessment. These tools are crucial for early detection of the disease, assessing its progression, stratifying risk, and guiding management decisions, including the timing of prophylactic surgical intervention.

- **Imaging Techniques:** Imaging is fundamental for determining the presence and progression of aortic disease, various modalities are used, each with specific strengths:
    - **Computed Tomography (CT) / Computed Tomographic Angiography (CTA):** CT is widely adopted for assessing suspected aortic pathology and for periprocedural vascular evaluation, often supplanting diagnostic catheter angiography, it offers rapid acquisition of intuitive, high-resolution 3-dimensional (3D) imaging data set, CT has very high sensitivity and specificity for acute aortic syndromes (AAS), including aortic dissection, intramural hematoma (IMH), and penetrating atherosclerotic ulcer (PAU). It can identify concomitant coronary involvement, branch vessel involvement, and hemopericardium. For suspected AAS, a noncontrast CT series is typically obtained first, followed by arterial phase contrast-enhanced images (CTA) extending from the thoracic inlet to the femoral arteries to define the full extent of any dissection and guide therapy. CT is generally preferred for surveillance imaging after thoracic endovascular aortic repair (TEVAR). It is also preferred when an abdominal aortic aneurysm (AAA) reaches the threshold for intervention, to confirm diameters and detail anatomy for preoperative planning.
    - **Magnetic Resonance Imaging (MRI) / Magnetic Resonance Angiography (MRA):** MRI is a reasonable alternative to CT for assessing thoracic aortic anatomy and diameters, ECG-gated MRI techniques minimize motion artifact and allow precise measurement of aortic root and ascending aortic dimensions,

MRI can be used for longitudinal surveillance of aortic dimensions and even if generally more limited by metallic artifact than CT, MRI is a reasonable alternative for surveillance after thoracic aorta repair. Non-contrast MRA can be used for follow-up and detection of endoleaks after endovascular aortic repair.

- **Echocardiography (Transthoracic Echocardiography - TTE and Transesophageal Echocardiography - TEE):** TTE is the most common imaging modality used in the initial nonemergency assessment of the thoracic aorta, it is particularly useful for imaging the aortic root and ascending aorta, and for delineating aortic valve anatomy and function. TTE is portable and can be performed at the bedside with high spatial and temporal resolution, as seen previously for the other imaging tools TEE is useful in the longitudinal surveillance of aortic root and ascending aortic dilation if well visualized. TEE provides high-resolution images of most of the thoracic aorta and is very useful in detailing aortic valve anatomy and function

- **Intravascular Ultrasound (IVUS):** IVUS is an endovascular technology providing high-resolution intraluminal imaging, it is useful in guiding endovascular management of complex aortic pathologies and in the setting of aortic dissection to distinguish true and false lumen anatomy and assess landing zones, it can also be used to guide stent deployment and reduce contrast volume.

- **Clinical Evaluation:** A detailed medical history and physical examination are essential components of the initial evaluation. Family history of aortic disease, known aortic valve disease, known aortic aneurysm, and previous aortic manipulation or surgery should be seen as warning signs suggesting a diagnosis of connective tissue diseases. High-risk physical examination features include pulse deficit and aortic diastolic murmur. Regarding clinical evaluation of subject with a suspected pathology associated with TAA, they should underwent a multidisciplinary evaluation that included cardiological, ophthalmological, internal medicine and genetic assessment.

- **Laboratory Tests or Biomarkers:** Traditional circulating biomarkers currently have limited support for diagnostic screening and decision-making, especially regarding the timing of intervention. However, some biomarkers can assist in identifying high-risk patients, establishing prognosis, and evaluating disease during follow-up. D-Dimer (DD) is a notable biomarker tested for identifying TAA patients at risk for dissection. While highly sensitive, it is largely unspecific. DD may also be used in prognosis prediction and monitoring adverse events in diagnosed dissection cases. Basic metabolic panels, cardiac biomarkers, troponin T, and complete blood count are part of laboratory evaluation in acute aortic pathologies, but are often insufficient and nonspecific for diagnosis.

Role of genetics in diagnosis and management

From the laboratory point of view, given that syndromic/non-syndromic TAA are most often inherited in an autosomal dominant pattern, molecular-genetic analysis represents a most valuable tool allowing early identification of affected individual as well as those subjects at higher risk of developing adverse outcomes in terms of aneurysm-growth speed and dissection (72). This is particularly relevant for TAAs involving the ascending aorta, whose etiology is predominantly linked to a crucial genetic component. In non-syndromic cases, features suggestive of a genetic etiology, even without syndromic signs, include young age at presentation (<50 years old), multiple aneurysms or dissections, and aortic root aneurysm. Mutations are described to have variable penetrance depending on the TAA presentation, from almost 100% in MFS and 90% in LDS, to 50% in familial TAA and dissection (FTAAD) and BAV in the presence of ascending aortic aneurysm. In fact, in the case of FTAAD, the causal mutation is found in much fewer cases (<10%) than in MFS or LDS, this discrepancy also being evident at the phenotypic level, presenting with a different severity of clinical manifestations along with age of presentation or diagnosis. When features of a connective-tissue disorder are present, patients should undergo genetic counselling and testing where appropriate.

As mentioned in previous paragraphs, both MFS and LDS conditions lead to the overactivation of TGFβ signalling (mutations in the *FBN1* protein in MFS lead to the increased chemical availability of TGFβ). Collagen is a vital structural protein of the aortic wall, particularly type III collagen, which predominates in the aortic media and is synthesised by VSMCs. Collagen fibre strength is dependent on its cross-links formed between adjacent helical domains. A heterogeneous group of connective tissue disorders, many types of Ehlers-Danlos Syndromes (EDS) are known to cause serious vascular complications and aneurysmal disease, all of which are linked to the molecular structure and assembly of fibrillar collagen. According to the Villefranche nosology, the classic, hypermobile, vascular and kyphosclerotic types (formerly types I/II, III, IV and VI) are associated with aortic enlargement (73). Arterial rupture may occur with or without a preceding aneurysm. Given the extreme friability and fragility of aortic tissue, patients with type IV Ehlers-Danlos syndrome are at a greater risk of adverse outcomes following vascular surgery than patients with other connective tissue disorders. Median survival of patients is 48 years (74). Inheritance is autosomal dominant, and diagnosis is confirmed by abnormal type III collagen biosynthesis and/or the identification of a mutation in *COL3A1*: this is the only gene known to be associated with EDS vascular type. More than 70 mutations have been identified (75). Bicuspid aortic valve (BAV) disease is the most common cardiovascular malformation in humans (1-2%), with a gender bias of 2:1, males versus females (76). TAAs affect about 40% of patients with BAVs and have a considerable association with increased risk of dissection and rupture (77). BAV occurs as a result of defective endocardial endothelial-to-mesenchymal transition during embryonic development e a process that relies strongly on *NOTCH1* signalling. The association between BAV-related aortopathy and Notch 1 signalling has been noted though only a very small portion of patients with both BAV and TAA have any mutations in *NOTCH1* or any of the known aortopathy genes (78). Despite this, it is widely observed that the BAV-associated TAA syndrome follows an autosomal dominant pattern of inheritance, albeit with incomplete

penetrance and variable expressivity (79,80).

Table 3. Summary of principal genes associated with TAA phenotypes

Gene	Associated Protein	OMIM	Syndrome	Pathway
FBN1	Fibrillin-1	134797	MFS, MASS phenotype	Extracellular matrix proteins
COL3A1	Collagen 3 α-1	120180	EDS vascular type	
TGFBR1	TGFβ receptor-1	190181	LDS type 1	TGFB signalling pathway
TBFBR2	TGFβ receptor-2	190182	LDS type 2	
TGFB2	TGFβ-2	190220	LDS type 4	
TGFB3	TGFβ-3	190230	LDS type 5	
SMAD3	SMAD family member 3	603109	LDS type 3	
SMAD2	SMAD family member 2	601366	LDS type 6	
ACTA2	α-smooth muscle actin	102620	Familial aortic aneurysm with levido reticularis and iris floccule	Cytoskeletal/SM contraction apparatus proteins
MYH11	smooth muscle myosin	160745	Familial aortic aneurysm with patent ductus arteriosus	
PRKG1	protein kinase, cGMP dependent type I	176894	Familial aortic aneurysm and dissection	

The existence of hereditary TAA with no other syndromic manifestations was recognised over thirty years ago, though their increased recognition in recent years has stemmed from the ongoing discovery of novel causative genes. Termed Familial Thoracic Aortic Aneurysms and Dissection (or FTAAD), these conditions follow an autosomal pattern of inheritance with decreased penetrance and variable expression (81). A common collection of causative genes of FTAAD (*ACTA2*, *MYH11*, *MYLK*, *PRKG1*) all code for SMC contractile proteins (figure 3). In

normal subjects, SMCs express the smooth muscle-specific isoform of a-actin (encoded by *ACTA2*) that oligomerises to form thin filaments. Actomyosin contractility and VSMC linkage with the ECM are vital for appropriate aortic mechanical homeostasis, which relies on the cross-linkage between actin and myosin filaments (82).

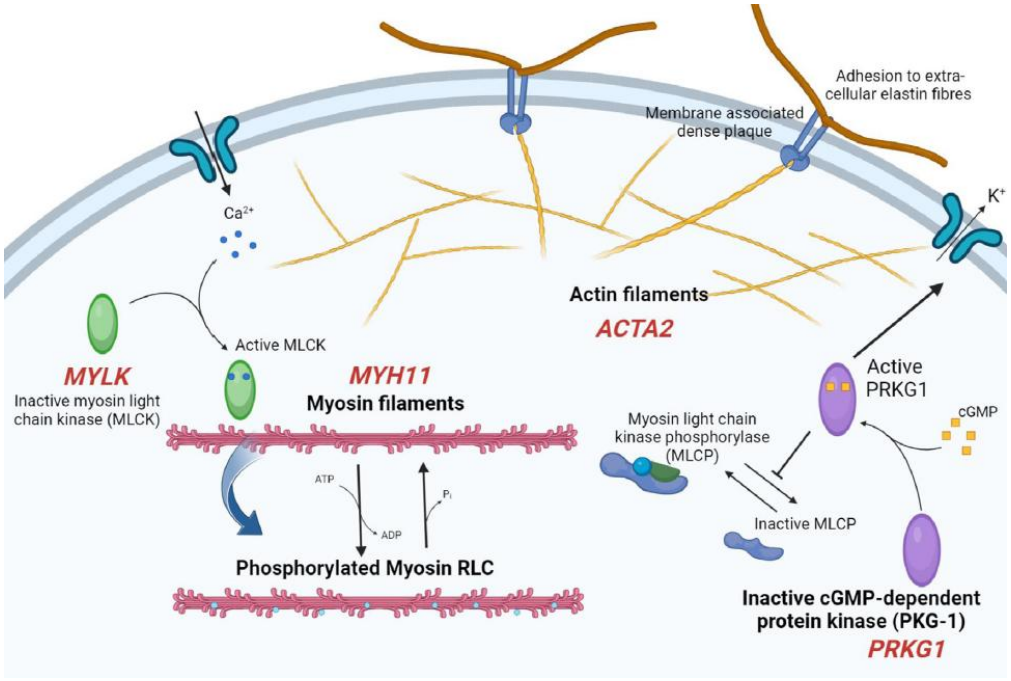

Figure 3. Signalling pathways involved in VSMC contraction/relaxation. Mutated genes causing heritable thoracic aortic disease (red font) disrupt critical proteins involved in SMC contraction. The pathway converges at the common step of regulatory light chain (RLC) phosphorylation. [The genetic basis of thoracic aortic disease: The future of aneurysm classification?, Hellenic Journal of Cardiology]

Clinical applicability of genetic testing for TAA and TAAD

Genetic testing for rare disease-causing variants in hereditary TAA and TAAD genes is available worldwide. Selecting patients suitable for testing should be considered when an adequate suspicion of hereditary aortopathy exists. Referrals for testing will be triaged by the Genomic Laboratory; testing should be targeted at those where a genetic or genomic diagnosis will guide management for the proband or family. The criteria used to select patients, as outlined in the National Genomic Medicine Service Directory, are based on the incidence of TAA/TAAD at a young age, the presence of a family history and clinical features of connective tissue disease. The rationale for genetic testing is crucial because individuals can be identified as at-risk for TAAD and associated mortality/ morbidity is preventable, including for potentially at-risk family members. Powerful information for aortic and other vascular disease management can also be collected (52). For the ease of understanding, the genetic basis of TAA and TAAD has been typically classified as syndromic (part of a set of clinical findings) or non-syndromic (occurring as an isolated finding), as it has been classified in much of the contemporary literature on this subject. However, the distinction between the two entities is becoming increasingly blurred: current data indicates that variants in hereditary TAA genes can lead to a phenotypic spectrum that ranges from syndromic to non-syndromic risk for TAA/TAAD. In addition, some

variants confer a high penetrant risk for disease, whereas other variants in the same gene confer a low penetrant risk for disease (83). Another important recent finding is that the frequency of VUSs identified in disease-associated genes in patients with TAAD was found to be significantly higher than in controls, with 30% of the cases having 1 to 3 VUSs. The burden of VUSs was the greatest for *ACTA2*, *TGFBR2*, *TGFBR1* and *MYLK*. Functional assays and bioinformatics analyses support the hypothesis that some of these VUSs are disease-predisposing variants that randomly trigger disease or when other risk factors are present (namely hypertension) but are not in isolation highly penetrant pathogenic variants. The future, therefore, lies in the improvement of classification for VUSs in known hereditary TAA/ TAAD genes so that accurate clinical assessment for the risk of TAAD in the general population can be conducted (84). Causal mutations are frequently identified in MFS and LDS, compared to FTAAD, where the causal mutation is identified in less than 10% of cases. The process of ascribing pathogenicity to a VUS is a complex process and should follow the ACMG guidelines (85).

Genetics' impact on prophylactic surgical intervention

Genetic variants and underlying genetic conditions significantly influence the recommended size thresholds for prophylactic surgical intervention for aortic disease, often necessitating surgery at smaller aortic diameters compared to the standard thresholds for sporadic aneurysms. The primary criterion for elective surgical repair of aneurysms of the aortic root or ascending thoracic aorta has traditionally been a maximum diameter of ≥5.5 cm (Figure 4), based on studies examining diameters at the time of adverse events and assuming a low operative mortality. However, aortic dissection can occur at diameters smaller than these recommended surgical thresholds, particularly in patients with heritable thoracic aortic disease (HTAD) (4).

- **Marfan Syndrome (MFS):** In patients with Marfan syndrome, aortic repair is recommended at a diameter of ≤5.0 cm. While the risk of aortic dissection is low when aortic diameters are <5.0 cm and managed with optimal medical therapy, the risk increases when the diameter is >5.0 cm and is higher in patients with a family history of aortic dissection or rapid aortic growth (86).

- **Loeys-Dietz Syndrome (LDS):** In patients with Loeys-Dietz syndrome, aortic dissection may occur at smaller aortic diameters than in Marfan syndrome, particularly those attributable to pathogenic variants in *TGFBR1*, *TGFBR2*, and *SMAD3*.

- **Nonsyndromic HTAD Related to Specific Genes (*ACTA2*, *PRKG1*, *MYH11*, *MYLK*, *LOX*):** These variants confer a highly penetrant risk for TAD, the decision regarding the timing of aortic repair is based on aortic diameter, age, family history, and the presence or absence of additional risk factors (87).

Other factors that can lower surgical thresholds in patients with genetic predispositions include rapid aortic growth, a family history of aortic dissection at a young age or small diameter, the presence of specific extra-aortic features, and pregnancy (4).

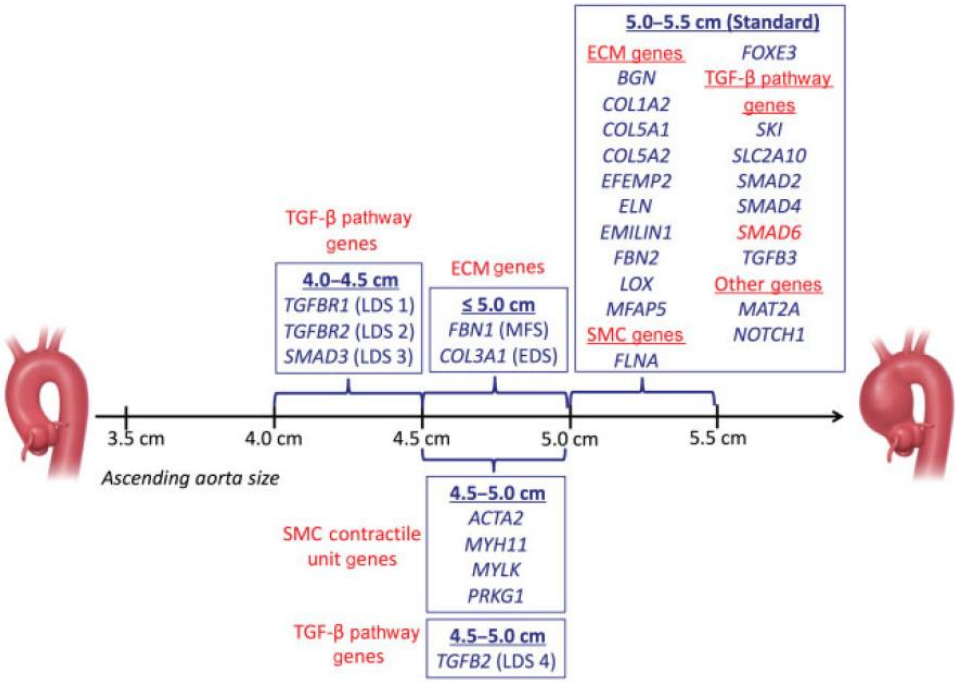

Figure 4. Ascending aorta dimensions for prophylactic surgical intervention. [Genes Associated with Thoracic Aortic Aneurysm and Dissection: 2018 Update and Clinical Implications, Aorta 2018]

2. PURPOSE OF THE STUDY AND PATIENT COHORT

This study aimed to match the molecular information obtained by next generation sequencing with the clinical characteristics of the patients attending the Regional Referral Centre for Marfan Syndrome and Related Disorders (Careggi Hospital, Florence) for differential diagnosis of aortopathy, particularly focusing on cardiovascular manifestations. Written informed consent was obtained from subjects included in the study, and the Careggi Hospital Ethics Committee approved the study. The experimental design envisaged the selection of subjects with pathogenic or probably pathogenic variants according to the American College of Medical Genetics and Genomics (ACMG)(85) classification in the *FBN1* gene and in the genes responsible for the autosomal dominant forms of LDS (*TGFBR1*, *TGFBR2*, *SMAD2*, *SMAD3*, *TGFB2*, *TGFB3*). Variants of uncertain significance, although of great interest, were not selected due to the difficulty in some cases of reclassifying them by segregation analysis or functional studies.

3. MATERIALS AND METHODS

Manual DNA extraction

Blood is taken in Vacutainer® tubes containing the anticoagulant EDTA. The tubes must be stored, until extraction, at -20°. It is, of course, essential to exercise great care and precision in the various steps of the operation, as good sample quality is essential to ensure reproducibility and reliability of the results of subsequent analyses.

DNA extraction was made Qiamp DNA Mini Kit (QIAGEN), this kit is for purification of total (genomic, mithocondrial and viral) DNA from whole blood, plasma, serum, buffy coat, lymphocytes and body fluids using a micorcentrifuge. The procedure is:

1. Pipet 20 µL QIAGEN Protease into the bottom of a 1,5 mL microcentrigue tube.

2. Add 200 µL sample to the microcentrifuge tube.

3. Add 200 µL Buffer AL to the sample. Mix by pulse-vortexing for 15 seconds.

4. Incubate at 56°C for 10 minutes.

5. Briefly centrifuge the 1,5 mL microcentrifuge tube to remove drops from the inside of the lid.

6. Add 200 µL ethanol (96-100%) to the sample, mix again by pulse vortexing for 15 seconds and then briefly centrifuge the tube to remove drops from the inside of the lid.

7. Carefully apply the mixture from the previous step to the QIAmp Mini spin column (in a 2 mL collection tube) without wetting the rim. Close the cap and centrifuge at 6000 x g for 1 min. Place the QIAmp Mini spin column in a clean 2 mL collection tube and discard the tube containing the filtrate.

8. Carefully open the QIAamp Mini spin column and add 500 µL Buffer AW1 without wetting the rim. Close the cap and centrifuge at 6000 x g for 1 min. Place the QIAamp Mini spin column in a clean 2 mL collection tube and discard the collection tube containing the filtrate.

9. Carefully open the QIAamp Mini spin column and add 500 µL Buffer AW2 without wetting the rim. Close the cap and centrifuge at full speed for 3 min.

10. Recommended: Place the QIAamp Mini spin column in a new 2 mL collection tube and discard the old collection tube with the filtrate. Centrifuge at full speed for 1 min. This step helps to eliminate the chance of possible Buffer AW2 carryover.

11. Place the QIAamp Mini spin column in a clean 1.5 mL microcentrifuge tube and discard the collection tube containing the filtrate. Carefully open the QIAamp Mini spin column and add 200 µL Buffer AE or distilled

water. Incubate at room temperature (15–25°C) for 1 min, and then centrifuge at 6000 x g for 1 min.

Qualitative And Quantitative Evaluation Using Nanodrop One

Before taking pedestal measurements with the NanoDrop One instrument, lift the arm of the instrument and clean the upper and lower pedestals. Clean the pedestals at least with a new laboratory wipe.

For measuring nucleic acid:

1. From the Home screen, select the Nucleic Acids tab and select dsDNA, ssDNA or RNA, depending on the samples to be measured.
2. Pipette 1-2 µL of blanking solution onto the lower pedestal and lower the arm.
3. Tap Blank and wait for the measurement to be completed.
4. Lift the arm and clean the two pedestals with a new laboratory wipe.
5. Pipette 1-2 µL of sampling solution onto the pedestal and lower the arm.
6. Start measuring the sample: If Auto-Measure is activated, lower the arm.
7. When you have finished measuring samples, tap End Experiment.
8. Lift the arm and clean the two pedestals with a new wipe.

DNA quantification with Qubit® Fluorometric Method

After quantifying the genomic DNA (gDNA) samples by Nanodrop measurement, noting the DNA concentration, 260/280 and 260/230 absorbance ratios, re-quantify using the Qubit® Fluorometric Method. Make sure you have the required materials available including the 0.5 ml Qubit® assay tubes, the reagent and buffer in the kit as well as the standards for calibrating the instrument. Prepare the working solution by diluting the Qubit® dsDNA HS Reagent at a ratio of 1:200 in the Qubit® dsDNA HS Buffer. Add 190 µL of the working solution to the cones used for standards, then add 10 µL of Qubit® standard to the respective cone, vortex for 2-3 seconds taking care not to form bubbles. Prepare the cones for the samples taking into account that the sum of the volumes between working buffer and sample must be exactly 200 µL; therefore the sample must be between 1-20 µL and the corresponding volume of working buffer between 180-199 µL, mix by vortexing for 2-3 seconds. Leave the cones to incubate for two minutes at room temperature, then first read the standards and then the samples on the Qubit® fluorometer.

Library Preparation Using Agilent Sureselect Protocol

Step 1. Fragment and adaptor-tag the genomic DNA samples

In this step, the gDNA is enzymatically fragmented and adaptors are added to ends of the fragments in a single reaction. For each DNA sample to be sequenced, prepare 1 library. At this stage also thaw the DMSO that will be used later in the PCR step.

1. Verify that the SureSelect QXT Stop Solution contains 25% ethanol, by referring to the container label and the instructions below. Before the first use of a fresh container, add 1.5 ml of ethanol to the provided bottle containing 4.5 ml of stop solution, for a final ethanol concentration of 25%. Seal the bottle then vortex well to mix. After adding the ethanol, be sure to mark the label for reference by later users.

2. Prepare reagents for the purification protocols

3. Quantify and dilute gDNA samples using two serial fluorometric assays. Adjust each gDNA sample with nuclease-free water to a final concentration of 25 ng/µl in a LoBind tube.

4. Before use, vortex the SureSelect QXT Buffer and SureSelect QXT Enzyme Mix ILM tubes vigorously at high speed. Note that the SSEL QXT Buffer is viscous and thorough and vigorous mixing is critical for optimal fragmentation.

5. Set up the fragmentation reactions on ice using a PCR plate or strip tube. Components must be added in the order listed below. Do not pre-mix the SureSelect QXT Buffer and Enzyme Mix.

    a. To each sample well, add 17 µl of SureSelect QXT Buffer.

    b. Add 2 µl of each DNA sample to its assigned sample well. While dispensing the DNA, be sure to place the pipette tip at the bottom of the well.

    c. Add 2 µl of SureSelect QXT Enzyme Mix, ILM to each sample well. While dispensing the enzyme mixture, place the pipette tip at the bottom of the well. After dispensing of the 2 µl of enzyme mix, pipette up and down 8 to 10 times to ensure complete transfer of the viscous solution to the well.

6. Seal the wells, briefly spin, then mix thoroughly by vortexing the plate or strip tube at high speed for 20 seconds.

7. Briefly spin the samples, then immediately place the plate or strip tube in the thermal cycler with the program for DNA Fragmentation (Table 4).

Table 4. Thermal cycler program for DNA fragmentation

Step	Temperature	Time
Step1	45°C	10 minutes
Step2	4°C	1 minutes
Step3	4°C	Hold

8. When the thermal cycler has completed the 1-minute incubation at 4°C, immediately place the samples on ice and add 32 µl of 1X SureSelect QXT Stop Solution (containing 25% ethanol) to each fragmentation reaction.

Seal the wells with fresh caps, then vortex at high speed for 5 seconds. Briefly spin the plate or strip tube to collect the liquid. Incubate the samples at room temperature for 1 minute.

Step 2. Purify the adaptor-tagged library using AMPure XP beads

Before you begin, verify that the AMPure XP beads have been incubated at room temperature for at least 30minutes and that fresh 70% ethanol has been prepared

1. Verify that the AMPure XP bead suspension has been well mixed and appears homogeneous and consistent in color.

2. Add 52 µl of the homogeneous bead suspension to each well containing the DNA samples. Seal the wells with fresh caps, then vortex for 5seconds. Briefly spin the samples to collect the liquid, without pelleting the beads. Check that the beads are in a homogeneous suspension in the sample wells. Each well should have a uniform color with no layers of beads or clear liquid present.

3. Incubate samples for 5 minutes at room temperature.

4. Put the plate or strip tube on the magnetic stand at room temperature. Wait for the solution to clear (approximately 3 to 5 minutes).

5. While keeping the plate or tubes in the magnetic stand, carefully remove and discard the cleared solution from each well. Do not disturb the beads while removing the solution.

6. Continue to keep the plate or tubes in the magnetic stand while you dispense 200 µl of fresh 70% ethanol in each sample well.

7. Wait for 1 minute to allow any disturbed beads to settle, then remove the ethanol.

8. Repeat step 6 and step 7 once for a total of two washes. Make sure to remove all of the ethanol at each wash step.

9. Dry the samples on the thermal cycler (with lid open) at 37°C for 1 to 3 minutes. Do not overdry the samples.

10. Add 11 µl of nuclease-free water to each sample well.

11. Seal the sample wells with fresh caps, then mix well on a vortex mixer and briefly spin the plate or tubes to collect the liquid.

12. Incubate for 2 minutes at room temperature.

13. Put the plate or tubes in the magnetic stand and leave for 2 minutes or until the solution in each well is clear.

14. Remove each cleared supernatant (approximately 10 µl) to wells of a fresh plate or strip tube and keep on ice. You can discard the beads at this time.

Step 3. Amplify the adaptor-tagged DNA library

In this step, the adaptor-tagged gDNA library is repaired and PCR-amplified.

1. Prepare the appropriate volume of PCR reaction mix, as described in the table below. Mix well on a vortex mixer.

Table 5. Preparation of pre-capture PCR Reaction mix

Reagent	Volume for 1 reaction
Nuclease-free water	25 µl
Herculase II Fusion DNA Polymerase	1 µl
Herculase II 5× Reaction Buffer	10 µl
100 mM dNTP Mix (25 mM each dNTP)	0.5 µl
SureSelect QXT Primer Mix	1 µl
DMSO	2.5 µl
Total	40 µl

2. Add 40 µl of the pre-capture PCR reaction mix prepared in step 1 to each 10-µl purified DNA library sample. Seal the wells with fresh caps and mix by vortexing gently for 5 seconds. Spin samples briefly to collect the liquid.

3. Incubate the plate in the thermal cycler (with the heated lid ON) and run the program in Table 6.

Table 6. Thermal cycler program for pre-capture PCR

Segment number	Number of Cycles	Temperature	Time
1	1	68°C	2 minutes
2	1	98°C	2 minutes
3	8	98°C	30 seconds
		57°C	30 seconds
		72°C	1 minute
4	1	72°C	5 minutes
5	1	4°C	Hold

Step 4. Purify the amplified library with AMPure XP beads

Before you begin, verify that the AMPure XP beads have been kept at room temperature for at least 30minutes and that fresh 70% ethanol has been prepared

1. Mix the AMPure XP bead suspension well so that the suspension appears homogeneous and consistent in color.

2. Transfer the samples to room temperature, then add 50 µl of the homogeneous bead suspension to each sample well containing the 50-µl amplified DNA samples. Seal the wells with fresh caps, then vortex for 5seconds. Briefly spin the samples to collect the liquid without pelleting the beads. Check that the beads are in a homogeneous suspension in the sample wells. Each well should have a uniform color with no layers of beads or clear liquid present.

3. Incubate samples for 5 minutes at room temperature.

4. Put the plate or strip tube on the magnetic stand at room temperature. Wait for the solution to clear (approximately 3 to 5 minutes).

5. While keeping the plate or tubes in the magnetic stand, carefully remove and discard the cleared solution from each well. Do not disturb the beads while removing the solution.

6. Continue to keep the plate or tubes in the magnetic stand while you dispense 200 µl of fresh 70% ethanol in each sample well.

Wait for 1 minute to allow any disturbed beads to settle, then remove the ethanol.

7. Repeat step 6 and step 7 once for a total of two washes. Make sure to remove all of the ethanol at each wash step.

8. Dry the samples on the thermal cycler (with lid open) at 37°C for 1 to 3 minutes. Do not overdry the samples.

9. Add 13 µl of nuclease-free water to each sample well.

10. Seal the sample wells with fresh caps, then mix well on a vortex mixer and briefly spin the plate or tubes to collect the liquid.

11. Incubate for 2 minutes at room temperature.

12. Put the plate or tubes in the magnetic stand and leave for 2 minutes or until the solution in each well is clear.

13. Remove each cleared supernatant (approximately 13 µl) to wells of a fresh plate or strip tube. You can discard the beads at this time.

Step 5. Assess library DNA quantity and quality

Use a Bioanalyzer DNA 1000 chip and reagent kit. Perform the assay according to the Agilent DNA 1000 Kit Guide.

1. Set up the 2100 Bioanalyzer instrument as instructed in the reagent kit

guide.

2. Prepare the chip, samples and ladder as instructed in the reagent kit guide, using 1 µl of each sample for the analysis. Load the prepared chip into the instrument and start the run within five minutes after preparation.

3. Verify that the electropherogram shows the peak of DNA fragment size positioned between 245 to 325 bp. Variability of fragmentation profiles may be observed.

A peak DNA fragment size significantly less than 245 bp may indicate too little gDNA in the fragmentation reaction and may be associated with increased duplicates in the sequencing data. In contrast, a peak DNA fragment size significantly greater than 325bp may indicate too much gDNA in the fragmentation reaction and may be associated with decreased percent-on-target performance in sequencing results.

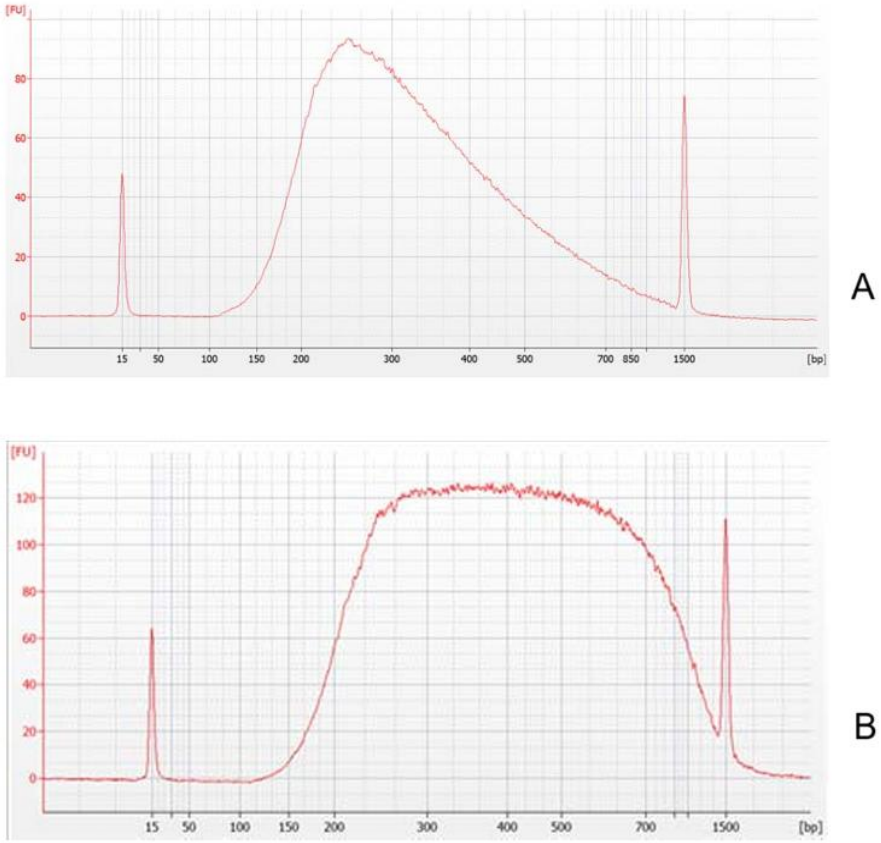

Figure 5. Representative sample electropherograms showing pre-capture analysis of amplified library DNA using the Agilent 2100 Bioanalyzer and a DNA 1000 Assay. (A) Electropherogram of a well fragmented sample. **(B)** Electropherogram of a sample associated with poor fragmentation, usually associated with too much gDNA in the reaction.

Step 6. Aliquot prepared DNA samples for hybridization

The amount of prepared gDNA library used in the hybridization reaction varies according to the design size of the probe used for hybridization as outlined in Table below.

Table 7. Amount of adaptor-tagged DNA libraries used for hybridization

Probe size	Amount of prepared gDNA library used in hybridization	Volume of prepared gDNA library samples added to hybridization
Probes > 3.0 Mb	750 to 1500 ng DNA	12 µl
Probes ≤ 3.0 Mb	500 to 750 ng DNA	12 µl

Step 7. Hybridize DNA Samples To The Probe

1. To each adaptor-tagged DNA sample well, add 5 µl of SureSelect QXT Fast Blocker Mix. Pipette up and down 8 to 10 times to mix, then cap the wells. Vortex at high speed for 5 seconds, then spin the plate or strip tube briefly. Sample wells now contain 17 µl of prepared DNA + Fast Blocker mixture.

2. Transfer the sealed prepared DNA + Blocker samples to the thermal cycler and start the program shown in Table 8, using a heated lid. The thermal cycler must be paused during Segment 3 to allow additional reagents to be added to the Hybridization wells

Table 8. Thermal cycler program for Hybridization

Segment #	Number of Cycles	Temperature	Time
1	1	95°C	5 minutes
2	1	65°C	10 minutes
3	1	65°C	1 minute (Pause cycler here for reagent addition)
4	60	65°C	1 minute
		37°C	3 seconds
5	1	65°C	Hold briefly until ready to begin capture

3. Prepare a 25% solution of SureSelect RNase Block (1 part RNase Block to 3 parts water), prepare the amount required for the number of hybridization reactions in the run, plus excess. Mix well. Keep the stock vial and diluted RNase Block on ice.

4. Prepare the Probe Hybridization Mix appropriate for your probe design size (< 3Mb) with the reagents listened in table 9.

Table 9. Preparation of Probe Hybridization Mix for probes <3 Mb

Reagent	Volume for 1 reaction
25% RNase Block solution	2 µl
Probe (with design <3 Mb)	2 µl
SureSelect Fast Hybridization Buffer	6 µl
Nuclease-free water	3 µl
Total	13 µl

5. Once the thermal cycler starts Segment 3 of the program in Table 8 (1minute at 65°C), pause the program. With the cycler paused, and while keeping the DNA + Blocker samples in the cycler, transfer 13µl of the room-temperature Probe Hybridization Mix.

6. Seal the wells with fresh domed strip caps. Make sure that all wells are completely sealed. Vortex at high speed for 5 seconds, and then spin the tubes or plate briefly and return the samples to the thermal cycler. The hybridization reaction wells now contain approximately 30µl.

7. Resume the thermal cycling program to allow hybridization of the prepared DNA samples to the probe.

Step 8. Prepare streptavidin-coated magnetic beads

1. Vigorously resuspend the Dynabeads MyOne Streptavidin T1 magnetic beads on a vortex mixer. The magnetic beads settle during storage.

2. For each hybridization sample, add 50 µl of the resuspended beads to wells of a fresh PCR plate or a strip tube.

3. Wash the beads:

    a. Add 200 µl of SureSelect Binding Buffer.

    b. Mix by pipetting up and down 10 times.

    c. Put the plate or strip tube into a magnetic separator device.

    d. Wait at least 5 minutes or until the solution is clear, then remove and discard the supernatant.

    e. Repeat step a through step d two more times for a total of 3 washes

4. Resuspend the beads in 200 µl of SureSelect Binding Buffer.

Step 9. Capture The Hybridized DNA Using Streptavidin-Coated Beads

1. After all streptavidin bead preparation steps are complete and with the hybridization thermal cycling program in the final 65°C hold segment, transfer the samples to room temperature.

2. Immediately transfer the entire volume (approximately 30 µl) of each hybridization mixture to wells containing 200 µl of washed streptavidin beads. Seal the wells with fresh caps.

3. Incubate the capture plate or strip tube on a 96-well plate mixer, mixing vigorously (at 1800 rpm), for 30 minutes at room temperature. Make sure the samples are properly mixing in the wells.

4. During the 30-minute incubation for capture, prewarm Wash Buffer 2 at 65°C as described below.

    a. Place 200-µl aliquots of Wash Buffer 2 in wells of a fresh 96-well plate or strip tubes. Aliquot 3 wells of buffer for each DNA sample in the run.

    b. Cap the wells with fresh domed caps and then incubate in the thermal cycler, with heated lid ON, held at 65°C until used in step 10.

5. When the 30-minute incubation period initiated in step 3 is complete, collect the liquid at the bottom of wells spinning the samples briefly

6. Put the plate or strip tube in a magnetic separator to collect the beads from the suspension. Wait 1 minute for the solution to clear, then remove and discard the supernatant.

7. Resuspend the beads in 200 µl of SureSelect Wash Buffer 1 (held at room temperature) by pipetting up and down 8 to 10 times. Make sure the beads are in suspension before proceeding.

8. Seal the wells with fresh caps, then mix by vortexing at high speed for 8 seconds. Collect the liquid at the bottom of wells by spinning the strip tubes.

9. Put the plate or strip tube in a magnetic separator. Wait 1 minute for the solution to clear, then remove and discard the supernatant.

10. Remove the plate or strip tubes from the magnetic separator and transfer to a rack at room temperature. Wash the beads with Wash Buffer 2, using the protocol steps below.

    a. Resuspend the beads in 200 µl of 65°C prewarmed Wash Buffer 2. Pipette up and down at least 10 times to resuspend the beads. Make sure the beads are in suspension before proceeding.

    b. Seal the wells with fresh caps and then vortex at high speed for 5

seconds. Collect the liquid at the bottom of wells by spinning the strip tubes.

c. Incubate the samples for 10 minutes at 65°C in the thermal cycler with the heated lid ON.

d. Put the plate or strip tube in the magnetic separator at room temperature

e. Wait 1 minute for the solution to clear, then remove and discard the supernatant.

f. Repeat step a through step e two more times for a total of 3 washes.

11. After removing the supernatant from the final wash, spin the samples briefly, return the plate or tubes to the magnetic stand, and then remove any remaining wash buffer droplets.

12. Add 23 µl of nuclease-free water to each sample well. Place the capture plate or strip tube on ice until PCR reactions are set up. Note that captured DNA is retained on the streptavidin beads during the post-capture amplification step. Do not separate the supernatant from the beads at this step.

Step 10. Amplify The Captured Libraries To Add Index Tags

In this step, the SureSelect- enriched DNA libraries are PCR amplified using the appropriate pair of dual indexing primers. Prepare one indexing amplification reaction for each DNA library.

1. Determine the appropriate index assignments for each sample. Use a different indexing primer combination for each sample to be sequenced in the same lane.

2. Prepare the appropriate volume of PCR reaction mix, as described in Table 10, on ice. Mix well on a vortex mixer.

Table 10. Preparation of post-capture PCR Reaction mix

Reagent	Volume for 1 reaction
Nuclease-free water	13.5 µl
Herculase II 5× Reaction Buffer	10 µl
100 mM dNTP Mix (25 mM each dNTP)	0.5 µl
Herculase II Fusion DNA Polymerase	1 µl
Total	25 µl

3. Obtain the plate or strip tube containing the bead-bound target-enriched DNA samples from ice. Add 25 µl of the PCR reaction mix prepared in

previous steps to the 23-µl of bead suspension in each sample well.

4. Add 1 µl of the appropriate P7 dual indexing primer (P7 i1 to P7 i12) to each PCR reaction mixture well. Add only one of the twelve possible P7 primers to each reaction well.

5. Add 1 µl of the appropriate P5 dual indexing primer (P5 i13 to P5 i20) to each PCR reaction mixture well. Add only one of the eight possible P5 primers to each reaction well.

6. Mix well by pipetting to ensure the beads are fully resuspended, then transfer the PCR plate or strip tube to a thermal cycler and run the PCR amplification program shown in Table 11.

7. When the PCR amplification program is complete, spin the plate or strip tube briefly. Remove the streptavidin-coated beads by placing the plate or strip tube on the magnetic stand at room temperature. Wait 2 minutes for the solution to clear, then remove each supernatant (approximately 50 µl) to wells of a fresh plate or strip tube. The beads can be discarded at this time.

Table 11. Post-Capture PCR cycling program

Segment #	Number of Cycles	Temperature	Time
1	1	98°C	2 minutes
2	Probes < 1 Mb: 14 Cycles	98°C	30 seconds
		58°C	30 seconds
		72°C	10 minutes
3	1	72°C	5 minutes
4	1	4°C	Hold

Step 11. Purify The Amplified Captured Libraries Using AMPure XP Beads

1. Let the AMPure XP beads come to room temperature for at least 30 minutes. Do not freeze the beads at any time.

2. Prepare 400 µl of fresh 70% ethanol per sample, plus excess, for use in step 8.

3. Mix the AMPure XP bead suspension well so that the suspension appears homogeneous and consistent in color.

4. Add 60 µl of the homogeneous AMPure XP bead suspension to each 50-µl amplified DNA sample in the PCR plate or strip tube. Seal the wells with

fresh caps, then vortex for 5 seconds. Briefly spin the samples to collect the liquid, without pelleting the beads. Check that the beads are in a homogeneous suspension in the sample wells. Each well should have a uniform color with no layers of beads or clear liquid present.

5. Incubate samples for 5 minutes at room temperature.
6. Put the plate or strip tube on the magnetic stand at room temperature. Wait for the solution to clear (approximately 3 to 5 minutes).
7. While keeping the plate or tubes in the magnetic stand, carefully remove and discard the cleared solution from each well. Do not disturb the beads while removing the solution.
8. Continue to keep the plate or tubes in the magnetic stand while you dispense 200 µl of fresh 70% ethanol in each sample well.
9. Wait for 1 minute to allow any disturbed beads to settle, then remove the ethanol.
10. Repeat step 8 and step 9 once for a total of two washes. Make sure to remove all of the ethanol at each wash step.
11. Dry the samples on the thermal cycler (with lid open) at 37°C for 1 to 3 minutes. Do not overdry the samples.
12. Add 25 µl of nuclease-free water to each sample well.
13. Seal the sample wells, then mix well on a vortex mixer and briefly spin the plate to collect the liquid.
14. Incubate for 2 minutes at room temperature.
15. Put the plate in the magnetic stand and leave for 2 minutes or until the solution is clear.
16. Remove the cleared supernatant (approximately 25 µl) to a fresh LoBind tube. You can discard the beads at this time.

Step 12. Assess Indexed Library DNA Quantity And Quality

Use the Bioanalyzer High Sensitivity DNA Assay to analyze the amplified indexed DNA. Perform the assay according to the High Sensitivity DNA Kit Guide.

1. Set up the 2100 Bioanalyzer instrument as instructed in the reagent kit guide.
2. Prepare the chip, samples and ladder as instructed in the reagent kit guide, using 1 µl of each sample for the analysis.
3. Load the prepared chip into the instrument and start the run within five minutes after preparation.
4. Verify that the electropherogram shows the peak of DNA fragment size positioned between 325 and 450 bp.

Sample Preparation For Sequencing On The Illumina Miseq Platform

Pool samples for multiplexed sequencing

Before sequencing, it is necessary to prepare a pool of the indexed post-capture libraries with a final concentration of 20nM (Vf=100µl) so that each sample is present in equimolar amounts within the pool. The following formula can be used for calculation:

$$\text{Volume of Index} = \frac{V(f) \times C(f)}{\# \times C(i)}$$

where $V(f)$ is the final desired volume of the pool,
$C(f)$ is the desired final concentration of all the DNA in the pool
$\#$ is the number of indexes, and
$C(i)$ is the initial concentration of each indexed sample.

Denaturation and dilution of libraries for sequencing on the MiSeq Illumina platform

Dilute the pool 20nM to a final concentration of 4nM. Prepare a 0.2N NaOH solution, Vf=1mL (800µl distilled water + 200µl NaOH 1.0N). Shake by inversion several times to homogenise the solution. The solution should be used within 12 hours of preparation. Thaw HT1 buffer at room temperature and store at 2-8°C until use.

For denaturation, add 5µl of 0.2N NaOH to 5µl of the 4nM pool. Vortex briefly and centrifuge at 280x g for 1 minute. Incubate 5 minutes at room temperature. Add 990 µl of pre-cooled HT1 buffer to the cone containing the denatured library pool. The result is 1 ml of a 20pM denatured library pool. Dilute the 20pM library pool with HT1 buffer to the desired concentration of 12pM.

Sequencing procedure on Illumina MiSeq platform

Thawing of the reagent cartridge is performed using a water bath containing deionised water at room temperature (MiSeq v3 cartridges: approximately 60 minutes). Remove the cartridge from the water bath and tap it gently on the bench to drain excess water from the cartridge base and dry the cartridge base. Turn the cartridge over 5 times to mix the thawed reagents, then visually inspect all positions to ensure they are thawed. Gently tap the cartridge on the bench to reduce air bubbles in the reagents. Place the reagent cartridge on ice or store it at 2-8 °C while waiting for the run to be set up. To sequence the SureSelectQXT libraries on Illumina's sequencing platforms, the custom sequencing primers are needed, these custom sequencing primers are provided at 100 nM and must be diluted in the corresponding Illumina primer solution, using the platform- specific instructions below:

Table 12. MiSeq platform custom sequencing primer preparation

Sequencing Read	Volume of SureSelectQXT Primer	Volume of Illumina TruSeq Primer	Total Volume	Final Cartridge Position
Read 1	3 µl SureSelect QXT Read Primer 1 (brown cap)	597 µl HP10 (well 12)	0.6 ml	well 18
Index	3 µl SureSelect QXT Index 1 Read Primer (clear cap)	597 µl HP12 (well 13)	0.6 ml	well 19
Read 2	3 µl SureSelect QXT Read Primer 2 (black cap)	597 µl HP11 (well 14)	0.6 ml	well 20

The "sample sheet" is then prepared using the Local Run manager interface, and index information is entered into the worksheet. The MiSeq Control Software interface provides commands to configure the instrument, set up and monitor runs and perform maintenance procedures. Run set-up includes loading the pre-filled reagent cartridge, buffer bottle and flow cell, with no further manual intervention. The kit includes a flow cell and the reagents required for sequencing: the PR2 bottle and the reagent cartridge, using radio frequency identification (RFID) for compatibility and accurate tracking of consumables. The pool is loaded onto the reagent cartridge before the start of the run and then automatically transferred to the flow cell after the start of the run. The MiSeq reagent cartridge is a disposable consumable consisting of small sealed reservoirs pre-filled with sufficient reagents for cluster generation and sequencing. Always perform an instrument wash after sequencing.

Bioinformatics And Statistical Analysis Of Illumina Sequencing Results

The analytical pipeline available in our laboratory, developed following guidelines suggested by the Broad Institute (88), commonly accepted as standard, was implemented and validated for targeted sequencing data analysis for diagnostic purposes. The quality of Fastq files was checked with FASTQC. Alignment to the human reference genome (Human GRCh37/hg19) was performed using BWA-MEM (89). GATK4 HaplotypeCaller was used for the variant calling step (90) and Ensembl Variant Effect Predictor (VEP) (91) with several plugins for variant annotation. A custom script was developed in R to check the coverage. Ninety-nine percent of targeted regions were covered. Variants were filtered according to the phred quality score (Q) ≥30 and a minimum coverage depth of 30x. Variants identified were prioritaized according to:

- MAF <0.01.
- the potential pathogenetic/modulatory role, according to variant

classification recommendation (85), literature genotype-phenotype association data or biological plausibility.

- in silico predictor tools (SIFT; PROVEAN; PolyPhen-2; MutationTaster; FATHMM; CADD; SPLICEAI; ASSP; NetGene2).
- type of genetic variants (missense, truncated variants, sinonimous variants, etc).
- localization (exonic, splicing regions variants).

The genetic data obtained from the next-generation sequencing experiment and the clinical data obtained through a retrospective analysis of the medical records of the subjects referred to our centre were merged into a database. The statistical analyses were performed using SPSS (version 28.0.1) software. Continuous variables were reported as median [interquartile range (IQR)], dichotomous variables (i.e. incidence of the event on the total number of cases) were reported as number (percentage). Comparison analyses for continuous variables were assessed by Mann Whitney test (independent samples), whereas dichotomous variables were compared by Fisher exact test. The p-value was considered significant if < 0.05.

4. RESULTS

Subjects

A total of 275 subjects were referred to our Center for aortopathy or suspected Heritable Thoracic Aorta Disorders (HTAD). Among them, 200 were males (72.7%) and 75 females (27.3%), with a median age of 48 years [interquartile range (IQR) 33 – 59] at their first visit (Table 13). The prevalence of traditional cardiovascular risk factor and thoracic aortic surgery are also reported in Table 13.

Table 13. Demographic and clinical parameters in the whole cohort and in the two groups of patients with aortopathy and with or without P/LP variants in *FBN1* and TGFβ pathway genes

	Whole cohort (n=275)	Patients with Aortopathy and without P/LP variants in FBN1 and TGFβ pathway genes (n = 238)	Patients with Aortopathy and with P/LP variants in FBN1 and TGFβ pathway genes (n = 37)	P value
Male Gender, n (%)	200 (72.7)	182 (76.4)	18 (48.6)	**< 0.001**
Age at first visit, yrs (IQR)	48 (33-59)	49 (36-59)	34 (20 – 48.5)	**< 0.001**
Height Adults (cm)	180 (173-186)	180 (172-186)	180 (175-190)	0.208
Height Paediatrics (cm)	183 (175-186)	184.5 (176.6-186)	179 (171-185)	0.342
Weight Adults (Kg)	76 (67-90)	76 (68-90)	75 (61-90)	0.539
Weight Paediatrics (kg)	57.5 (54-70)	63.5 (54.8-71.5)	55 (42-57)	0.058
Hypertension, n (%)	86 (31.2)	79 (33.1)	7 (18.9)	0.150
Diabetes, n (%)	4 (1.45)	3 (1.26)	1 (2.7)	0.436
Dyslipidaemia, n (%)	76 (27.6)	71 (29.8)	5 (13.5)	**<0.050**
Smoking Habitus, n (%)	66 (24)	64 (26.8)	2 (5.4)	0.398
Aortic Root z-score	2.73 (1.61-3.82)	2.56 (1.41-3.51)	3.55 (2.56-4.31)	**0.005**

Ascending Aorta Diameter, mm	38 (32-44)	38 (34-45)	31 (27-36)	**<0.001**
TAA Surgery, n (%)	57 (20.7)	43 (18.0)	14 (37.8)	**0.006**

Continuous variables are reported as median (IQR)

In the 238 patients, the aortic root z-score was significantly lower and the ascending aorta diameter was significantly higher than in the 37 patients with P/LP variants in *FBN1* and TGFβ pathway genes.

Of these subjects, 57 (20.7%) had undergone thoracic aortic surgery (Table 13). This included 33 individuals who had elective surgery (12%), while 23 subjects experienced a Type A or Type B aortic dissection (8.4%). Additionally, one subject had aortic coarctation with hypoplasia of the arch and underwent corrective surgery at the age of 10 years. The median age at the time of thoracic aorta surgery was 49 years (IQR 39 – 57). The median aortic root diameter among these patients was 41 mm (IQR 37 - 45 mm). Whether we normalise the measurements based on gender, age, height, and weight according to Z-score (https://marfan.org/dx/z-score-adults/ and https://marfan.org/dx/zscore-children/), we find that the average z-score for the aortic root is 2.73 (IQR 1.61-3.82).

Among these subjects, those showing the presence of at least one pathogenic (P) or likely pathogenic (LP) variants in the *FBN1* gene or TGFβ pathway genes (*TGFBR1, TGFBR2, SMAD2, SMAD3, TGFB2, TGFB3*) consist of 37 patients (13.4%), of which 29 with variants into the *FBN1* gene (15 variants classified as LP and 15 variants classified as P, one patient had 2 variants in the *FBN1* gene), 7 with variants in the *SMAD3* gene (5 variants classified as LP and 2 variants classified as P) and one with a LP variant in the *TGFB3* gene.

According to family history, clinical manifestation and genetics datum, n=27 subjects were diagnosed with Marfan syndrome, n=8 subjects were diagnosed with Loeys-Dietz syndrome, n=1 patient was diagnosed with MASS (Mitral valve prolapse, Aortic dilatation, Skeletal abnormalities, and Skin striae syndrome), and n=1 patient was diagnosed with Ectopia Lentis.

Concerning the 238 patients with aortopathy arrived to the attention of the Referral Center without causative mutations in *FBN1* and TGFbeta pathway genes, n=33 patients showed the following diagnoses: n=6 Marfan Syndrome, n=5 MASS, n=3 Familial Aortic Aneurysm/Dissection, n=15 Bicuspid Aortic Valve, n=2 vascular Ehlers Danlos Syndrome, n=1 Hypermobility Spectrum Disorder, n=1 Shprintzen-Goldberg Syndrome, and n=205 apparently isolated aortopathy.

The 37 patients included 18 males (48.6%) and 19 females (51.4%); 30 were adults (81.1%), and 7 (18.9%) were paediatric patients (under 18 years of age at the first visit). The median age at the first visit was 34 years (IQR 20-48.5).

Differences between the group of subjects with aortopathy and with or without P/LP genetic variants in the abovementioned genes are reported in Table 13.

No differences between the two groups are showed for height in adults and paediatrics, as well as concerning weight in adults. A trend towards statistical

significance was observed concerning weight in paediatric patients (higher in patients without causative mutation in selected genes) (Table 13).

Concerning traditional cardiovascular risk factors, there is a statistical significant higher prevalence in the group without P/LP genetic variants for dyslipidemia and male gender and a trend for hypertension and smoking habit (Table 13).

We concentrated our attention on the 37 patients with P/LP genetic variants.

In Tables 14, 15, 16, 17, and 18 detailed information concerning the main demographic and vascular characteristics, skeletal manifestations, craniofacial manifestation, valve disorders, and other clinical manifestations, respectively, are reported in the population of 37 subjects.

Table 14. Main Demographic and vascular characteristics of the 37 identified subjects with suggestive variants in the genes associated with Marfan syndrome and Loeys Dietz syndrome

	Adults or Paediatrics	Gender	Diagnosis	Age First Visit (yrs)	Z-Score Aortic Root	Thoracic Aortic Surgery	Presence of Non-Aortic Vascular Phenotypes [§]
P001	Adult	Female	MFS	48	3.25	-	+
P002	Adult	Male	MFS	73	1.24	-	+
P003	Adult	Male	LDS	45		+	+
P004	Adult	Male	LDS	60		+	+
P005	Adult	Female	MFS	35	4.87	+	+
P006	Adult	Female	MFS	41		+	+
P007	Adult	Female	LDS	31	2.22	-	+
P008	Adult	Male	LDS	62		+	+
P009	Adult	Female	MFS	36	3.63	-	-
P010	Adult	Male	LDS	55		+	-
P011	Adult	Female	MFS	61	4.48	-	-
P012	Adult	Female	MFS	33		+	-
P013	Adult	Female	MFS	49	2.06 (post surgery)	+	-
P014	Paediatric	Female	MFS	16	4.00	-	-
P015	Adult	Male	MFS	42	6.17	+	-
P016	Adult	Female	MFS	20	2.67	-	-

P017	Paediatric	Male	MFS	16	.24	-	-
P018	Adult	Female	Ectopia Lentis	63	.36	-	-
P019	Paediatric	Male	MFS	11	4.32	-	-
P020	Adult	Female	MFS	20	2.93	-	-
P021	Adult	Female	MFS	22	4.20	-	-
P022	Adult	Female	MFS	27	4.56	-	-
P023	Adult	Male	MFS	34	4.31	-	-
P024	Adult	Female	MFS	27	4.11	-	-
P025	Adult	Male	MFS	13	5.99	+	-
P026	Adult	Male	LDS	38	1.99	-	-
P027	Adult	Male	MFS	23	3.39	-	-
P028	Adult	Male	MFS	31	6.17	-	-
P029	Adult	Female	MFS	27	3.65	-	-
P030	Adult	Female	MFS	40	2.73	-	-
P031	Paediatric	Male	MASS	12	1.80	-	-
P032	Paediatric	Male	MFS	7		+	-
P033	Adult	Female	LDS	52	3.48	+	-
P034	Adult	Female	MFS	48		+	-
P035	Adult	Male	LDS	64	6.02 (post surgery)	+	-
P036	Paediatric	Male	MFS	14	2.73	-	-
P037	Paediatric	Male	MFS	3	2.53	-	-

§ Non-aortic Vascular Phenotypes include: Hemorrhagic stroke, Carotid artery dissection, Heart Failure, STEMI, Cardiac Arrest, Cardioversion.

Table 15. Skeletal manifestations in the population

Skeletal Manifestations	Patients N out of 37
Thumb Sign*, n (%)	15 (40.5)
Wrist Sign*, n (%)	13 (35.1)
Arachnodactyly, n (%)	9 (24.3)
Pectus Carinatum*, n (%)	17 (45.9)
Pectus Excavatum*, n (%)	13 (35.1)
Chest Wall Asymmetry*,	6 (16.2)

n (%)	
Hindfoot Deformity*, n (%)	10 (27.0)
Flat Foot*, n (%)	17 (45.9)
Spontaneously Occurring Pneumothorax*, n (%)	1 (2.7)
Scoliosis*, n (%)	22 (59.4)
Thoracolumbar Kyphosis *, n (%)	12 (32.4)
Reduced Elbow*, n (%)	6 (16.2)

* manifestations included in systemic score (Loeys Dietz et al. J Med Genet 2010)

Table 16. Craniofacial Manifestation in the population

Craniofacial	Patients N out of 37
Dolichocephaly*,, n (%)	18 (48.6)
Downward Slanting Palpebral Fissures*, n (%)	6 (16.2)
Enophthalmos*, n (%)	4 (10.8)
Retrognathia*, n (%)	13 (35.1)
Malar Hypoplasia*, n (%)	1 (2.7)

* manifestations included in systemic score (Loeys Dietz et al. J Med Genet 2010); 1 point in the systemic score is assigned based upon facial characteristics if the patient shows ≥3 facial features.

Table 17. Valve Disorders in the population

Valve Disorders	Patients out of 37
Mitral insufficiency, n (%)	11 (29.7)
- **Mild**	8 (21.6)
- **Moderate**	2 (5.4)
- **Severe**	1 (2.7)
Mitral Valve Prolapse (MVP)*, n (%)	15 (40.5)
Valve Flattering, n (%)	6 (16.2)
Mitral Surgery, n (%)	3 (8.1)
Mitral Annular Disjunction (MAD), n (%)	4 (10.8)
Bicuspid Aortic Valve (BAV), n (%)	1 (2.7)

* manifestations included in systemic score (Loeys Dietz et al. J Med Genet 2010)

Table 18. Other Clinica Manifestation

Valve Disorders	Patients out of 37
Skin Striae*, n (%)	21 (56.8)
Myopia ≥ 3 dioptres*, n (%)	12 (32.4)
Dural Ectasia*, n (%)	7 (16.2)

* manifestations included in systemic score (Loeys Dietz et al. J Med Genet 2010)

In the 37 patients, the median Systemic Score according to the updated Ghent Nosology classification (12) is 7.0 (IQR 3.5-9.0), while the median Beighton Score is 0 (Min 0 - Max 5). Whether systemic score was addressed according to diagnosis, the major criterium of ≥7 systemic manifestations was reached in a higher percentage of MFS [15 out of 27 (55.5%)] with respect to LDS patients [3 out of 8 (37.5%)] (p= 0.369).

Table 19 displays the available values of pre-surgery aortic diameters in patients by diagnosis. For part of patients undergoing surgery in emergency due to acute dissection no data on pre-surgery diameters are available.

Among the 37 subjects, 14 underwent thoracic aorta surgery (37.8%), with 9 cases exibiting dissection and 5 elective surgery. Among the 9 dissections, 8 occurred in the ascending aorta and are thus classified as type A dissections, one occurred in the descending aorta and is classified as type B. In table 20, the distribution of surgery and dissection according to MFS or LDS diagnosis is shown.

Similar results are observed for thoracic aorta diameters at different levels between MFS and LDS patients (Table 19), but considering z-score values representative of the deviance from normality according to age, BMI and gender, MFS patients showed higher median values (3.82, range 0.24-6.17) than LDS (2.22, range 1.99-3.48) (Table 19). The percentage of MFS patients with a Z-score >2 (major criterium for MFS diagnosis) is 91.3% while was 75% for LDS patients (Table 20).

Table 19. Aortic measurements in MFS and LDS patients

Diagnosis		Aortic Root (mm)	N valid values	Z-Score Aortic Root	N valid values	ascending thoracic aorta (mm)	N valid values
MFS	Median	40.50	22	3.82	22	30.00	17
(N = 27)	Range	26-52		0.24-6.17		21-42	
LDS	Median	39.00	3	2.22	3	31.00	1
(N = 8)	Range	36-41		1.99-3.48		NA	

Total (N = 35)	Median	40.00	25	3.48	25	30.00	18
	IQR	36.6-43.0		2.53-4.32		25.0-36.0	

Table 20. Thoracic aortic phenotypes in the 37 patients

Diagnosis	TAA (Z-score > 2)	Aortic Surgery	Type A aortic dissection	Type B aortic dissection	Elective surgery
MFS (N = 27)	21/23 pt (91.3%)	8/27 pt (29.6%)	4/8 pt (50%)	1/8 pt (12.5%)	3/8 pt (37.5%)
MASS (N = 1)	0	0	0	0	0
LDS (N = 8)	3/4 pt (75%)	6/8 pt (75%)	4/6 pt (66.7%)	0/6 pt (0%)	2/6 pt (33.3%)
Ectopia Lentis (N = 1)	0	0	0	0	0

pt=patient

In Table 21 non-aortic vascular manifestations of the 37 patients were described: n=8 subjects had non-aortic vascular manifestations; n=1 subject had both ST-Elevation Myocardial Infarction (STEMI) and carotid artery dissection (the only one with two manifestations); n=1 subject had a haemorrhagic stroke; n=1 subject had only carotid artery dissection; n=2 subjects displayed heart failure; n=1 subject had cardiac arrest; n=1 subject had non ST-Elevation Myocardial Infarction (NSTEMI); and n=1 subject had cardioversion for atrial fibrillation.

Table 21. Non-aortic vascular manifestations in the 37 patients

Non-Aortic Vascular Manifestations	N patients out of 37
Hemorrhagic stroke, n (%)	1 (2.7)
Carotid artery dissection, n (%)	2 (5.4)
Heart Failure, n (%)	2 (5.4)
NSTEMI, n (%)	1 (2.7)
STEMI, n (%)	1 (2.7)
Cardiac Arrest, n (%)	1 (2.7)
Cardioversion for atrial fibrillation, n (%)	1 (2.7)

Patients with Pathogenic or Likely Pathogenic variants in the *FBN1* gene

Thirty Likely Pathogenic (LP) or Pathogenic (P) variants falling in the *FBN1* gene were found in 29 patients. Among these variants, 15 are missense variants (50%), 8 are frameshift variants (26.6%), 4 are nonsense variants (13.3%), 2 are splice-site variants (6.7%) and 1 is an in-frame insertion (3.3%) (Figure 6).

All variants with ACMG (American College of Medical Genetics) classification (85) and applied criteria are listed in Table 22.

Among variants identified, two LP missense variants were found in the same subject (P011, Table 22). Seven out of 15 missense variants (46.7%) are aminoacidic substitution involving highly conserved Cysteine residues, while the other 8 missense variants involved different aminoacids.

Fourteen out of 30 *FBN1* variants (46.7%) are mutations determining the introduction of a premature stop codon or a defect in the mRNA maturation process potentially associated with haploinsufficiency (HI) and 16 (53.3%) are dominant-negative variants (DN), among which 2 are present in the same subjects (P011, Table 22). Thirteen out of the 16 DN variants (81.2%) fall into EGF-Like domains, 1 DN variant falls into the TB-3 domain, and 2 do not fall into any specific domain (Table 22).

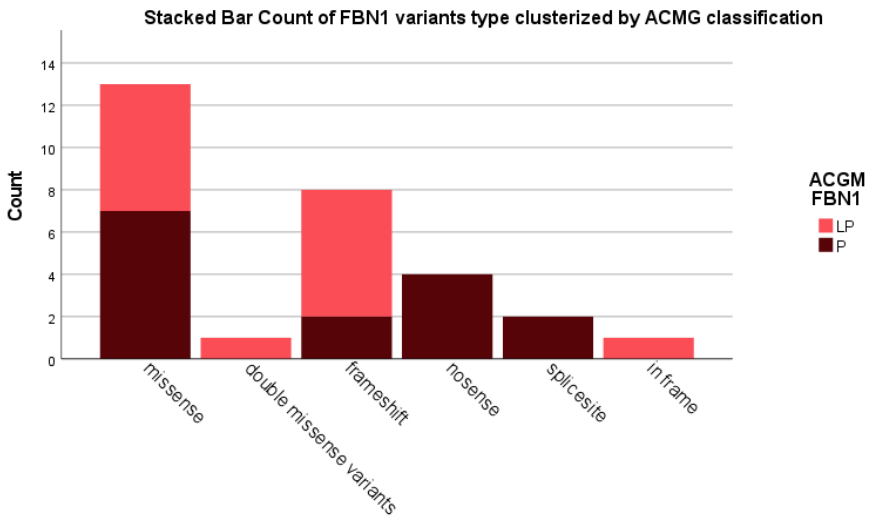

Figure 6. *FBN1* variants subtypes

Table 22. *FBN1* variants with ACMG classifications and applied criteria

ID case study	chr position	HGVS nomenclature (Coding DNA)	HGVS nomenclature (Protein)	ACGM	ACMG criteria
P001	chr15:48725111:T:G	c.6691A>C	p.(Lys2231Gln)	LP	PM1 strong, PM2 supporting, BP4 moderate
P002	chr15:48789533:G:T	c.2223C>A	p.(Asn741Lys)	LP	PS1 strong,PP3 strong,PM1 moderate,PM5 moderate,PM2 supporting,PP5 supporting
P005	chr15:48704896:G	c.8096del	p.(Pro2699HisfsTer53)	LP	PVS1 very strong, PM2 supporting
P006	chr15:48713848:C:T	c.7606G>A	p.(Gly2536Arg)	P	PP5 very strong,PM1 moderate,PM2 supporting, PP3 supporting
P009	chr15:48720587:C:T	c.6953G>A	p.(Cys2318Tyr)	P	PM5 Strong, PP3 strong,PM1 moderate,PP5 moderate,PM2 supporting
P011	chr15:48818371:C:T	c.944G>A	p.(Cys315Tyr)	LP	(1): PM1 moderate, PM5 moderate, PP3 moderate, PM2 supporting (2): PP3 strong,PM1 moderate,PM5 moderate,PM2 supporting
	chr15:48818376:G:C	c.939C>G	p.(Cys313Trp)	LP	
P012	chr15:48779377:TCAGCTCACAT	c.3474_3484del	p.(Glu1160ThrfsTer29)	LP	PVS1 very strong, PM2 supporting
P013	chr15:48805809:C:A	c.1525G>T	p.(Gly509Cys)	P	PS4 strong, PP1 supporting, PM1 moderate,PP2 supporting,PM2 moderate,PP3 moderate
P014	chr15:48741016:A:G	c.5620T>C	p.(Cys1874Arg)	P	PS4 strong, PM1 moderate, PP2 supporting, PM2 moderate
P015	chr15:48748888:G:A	c.5368C>T	p.(Arg1790Ter)	P	PS4 moderate, PVS1 very strong, PM2 moderate

P016	chr15:48905206:C:T	c.247+1G>A		P	PVS1 very strong, PP5 very strong, PM2 supporting
P017	chr15:48795999:G:A	c.2098C>T	p.(Pro700Ser)	LP	PM1 Moderate,PP2 supporting, PP3 moderate, PM2 moderate
P018	chr15:48741042::CAC	c.5592_5594dup	p.(Gln1864_Cys1865insTrp)	LP	PM1 strong, PM4 moderate, PM2 supporting
P019	chr15:48796013:G	c.2084del	p.(Pro695LeufsTer23)	LP	PVS1 very strong, PM2 supporting
P020	chr15:48903005:C:T	c.266G>A	p.(Cys89Tyr)	P	PP5 very strong, PM5 strong, PP3 strong, PM1 moderate, PM2 supporting
P021	chr15:48757883:ATCA	c.4821_4824del	p.(Ile1607MetfsTer32)	LP	PVS1 very strong, PM2 supporting
P022	chr15:48787702:C	c.2503del	p.(Glu835LysfsTer12)	LP	PVS1 very strong, PM2 supporting
P023	chr15:48756110:C:T	c.5051G>A	p.(Gly1684Glu)	LP	PM1 moderate, PP2 supporting,PM2 moderate, PP3 supporting
P024	chr15:48719928:AT	c.7039_7040del	p.(Met2347ValfsTer19)	P	PVS1 very strong, PS2 strong, PM2 moderate
P025	chr15:48936822:CT	c.144_145del	p.(Gly49ThrfsTer5)	LP	PVS1 very strong, PM2 supporting
P027	chr15:48902987:G:T	c.284C>A	p.(Ser95Ter)	P	PVS1 very strong, PM2 supporting
P028	chr15:48712949:A:G	c.7754T>C	p.(Ile2585Thr)	LP	PS4 moderate, PM1 moderate, PP2 supporting, PM2 moderate
P029	chr15:48738977:C:T	c.5714G>A	p.(Cys1905Tyr)	LP	PM1 moderate, PP2 supporting, PM2 moderate, PM5 moderate, PP3 moderate
P030	chr15:48779509:C:T	c.3463G>A	p.(Asp1155Asn)	P	PS3 supporting, PS2 strong, PM2 moderate, PM5 moderate, PP3 modarate, PP2 supporting
P031	chr15:48892369:G:A	c.409C>T	p.(Gln137Ter)	P	PVS1 very strong, PM2 supporting

P032	chr15:48782276:C:G	c.2855-1G>C		P	PVS1 very strong, PM2 supporting, PP5 supporting
P034	chr15:48808422:G:A	c.1285C>T	p.(Arg429Ter)	P	PVS1 very strong, PS4 moderate, PP1 supporting, PM2 moderate
P036	chr15:48719928:AT	c.7039_7040del	p.(Met2347ValfsTer19)	P	PVS1 very strong, PS2 strong, PM2 moderate
P037	chr15:48905255:A:G	c.199T>C	p.(Cys67Arg)	P	PM1 strong, PM5 strong, PP3 strong, PM2 supporting

HGVS (Human Genome Variation Society) nomenclature (https://hgvs-nomenclature.org/stable/)

Table 23 shows in the 29 *FBN1* patients the criteria for definition of diagnosis according to the updated Ghent nosology for Marfan Syndrome.

Table 23. Patients' variants and major criteria according to updated Ghent nosology

ID case study	HGVS coding	HGVS Protein	MFS Family History	Ectopia Lentis	Systemic score	Aortopathy	Diagnosis
P001	c.6691A>C	p.(Lys2231Gln)	NO	NEG	SCORE < 7	YES	MFS
P002	c.2223C>A	p.(Asn741Lys)	.	Bilateral	SCORE < 7	NO	MFS
P005	c.8096del	p.(Pro2699HisfsTer53)	YES	Monolateral	SCORE ≥ 7	YES	MFS
P006	c.7606G>A	p.(Gly2536Arg)	NO	NEG	SCORE ≥ 7	NO	MFS
P009	c.6953G>A	p.(Cys2318Tyr)	NO	NEG	SCORE ≥ 7	YES	MFS
P011	c.944G>A	p.(Cys315Tyr)	NO	NEG	SCORE ≥ 7	YES	MFS
P012	c.3474_3484del	p.(Glu1160ThrfsTer29)	NO	NEG	SCORE < 7	YES	MFS
P013	c.1525G>T	p.(Gly509Cys)	NO	NEG	SCORE < 7	YES	MFS
P014	c.5620T>C	p.(Cys1874Arg)	YES	NEG	SCORE ≥ 7	YES	MFS
P015	c.5368C>T	p.(Arg1790Ter)	NO	NEG	SCORE < 7	YES	MFS
P016	c.247+1G>A		NO	NEG	SCORE ≥ 7	YES	MFS
P017	c.2098C>T	p.(Pro700Ser)	NO	NEG	SCORE ≥ 7	NO	MFS
P018	c.5592_5594dup	p.(Gln1864_Cys1865insTrp)	NO	Surgery	SCORE ≥ 7	NO	Ectopia Lentis
P019	c.2084del	p.(Pro695LeufsTer23)	NO	Monolateral	SCORE ≥ 7	YES	MFS
P020	c.266G>A	p.(Cys89Tyr)	NO	Bilateral	SCORE ≥ 7	YES	MFS

P021	c.4821_4824del	p.(Ile1607MetfsTer32)	NO	NEG	SCORE ≥ 7	YES	MFS
P022	c.2503del	p.(Glu835LysfsTer12)	NO	NEG	SCORE < 7	YES	MFS
P023	c.5051G>A	p.(Gly1684Glu)	NO	NEG	SCORE < 7	YES	MFS
P024	c.7039_7040del	p.(Met2347ValfsTer19)	NO	NEG	SCORE ≥ 7	YES	MFS
P025	c.144_145del	p.(Gly49ThrfsTer5)	NO	NEG	SCORE ≥ 7	YES	MFS
P027	c.284C>A	p.(Ser95Ter)	YES	NEG	SCORE ≥ 7	YES	MFS
P028	c.7754T>C	p.(Ile2585Thr)	NO	NEG	SCORE < 7	YES	MFS
P029	c.5714G>A	p.(Cys1905Tyr)	NO	NEG	SCORE < 7	YES	MFS
P030	c.3463G>A	p.(Asp1155Asn)	NO	NEG	SCORE < 7	YES	MFS
P031	c.409C>T	p.(Gln137Ter)	NO	NEG	SCORE ≥ 7	NO	MASS
P032	c.2855-1G>C		YES	NEG	SCORE ≥ 7	NO	MFS
P034	c.1285C>T	p.(Arg429Ter)	NO	NEG	SCORE < 7	YES	MFS
P036	c.7039_7040del	p.(Met2347ValfsTer19)	NO	NEG	SCORE ≥ 7	YES	MFS
P037	c.199T>C	p.(Cys67Arg)	YES	Monolateral	SCORE < 7	YES	MFS

In Table 24, data concerning age, BMI, Z-score and systemic score according to the presence of DN or HI variants are reported.

Table 24. Differences in measurements between patients with mutations determining the introduction of a premature stop codon or a defect in the mRNA maturation process potentially associated with haploinsufficiency (HI) or with dominant-negative variants (DN)

	Patients (N=15) with DN variants	N valid values	Patients (N=14) with HI variants	N valid values	P value
Age in years at the first visit	36.00 (20.00-49.00)	15	22.50 (12.75-33.50)	14	**p = 0.046**
Height (cm)	178.0 (171.0-185.0)	15	182.0 (177.0-190.5)	13	p = 0.142
Weight (kg)	64.0 (50.0-78.0)	15	62.5 (55.25-85.75)	12	p = 0.614
BMI	19.75 (16.98-24.62)	15	18.10 (17.34-24.99)	12	p = 0.943
Z-Score Aortic Root	3.09 (1.85-4.07)	14	4.20 (2.73-4.87)	11	p = 0.095
Z-Score Aortic Root (only adults' patients)	3.25 (2.06-4.31)	11	4.38 (2.06-4.31)	10	p = 0.075
Systemic Score	5.00 (3.00-8.00)	15	8 (4.75-12.25)	14	**p = 0.041**

Continuous variables are reported as median (IQR) and comparisons were performed by the independent samples Mann-Whitney U test

Significantly higher values of systemic score in subjects with HI variants with respect to that observed in those with DN variants have been observed; as concerns age at first visit, subjects with HI variants were younger (Table 24).

The graphs below (Figures 7 and 8) show the boxplots of the systemic score and age at first visit in the two groups analysed.

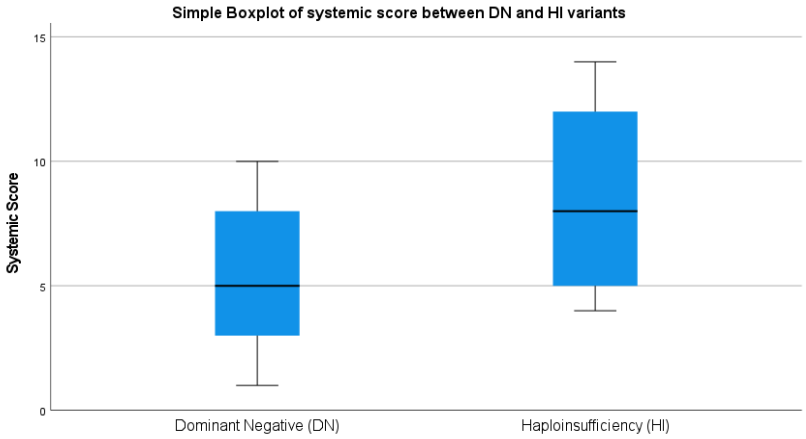

Figure 7. Boxplot of the systemic score between patients with DN and HI variants

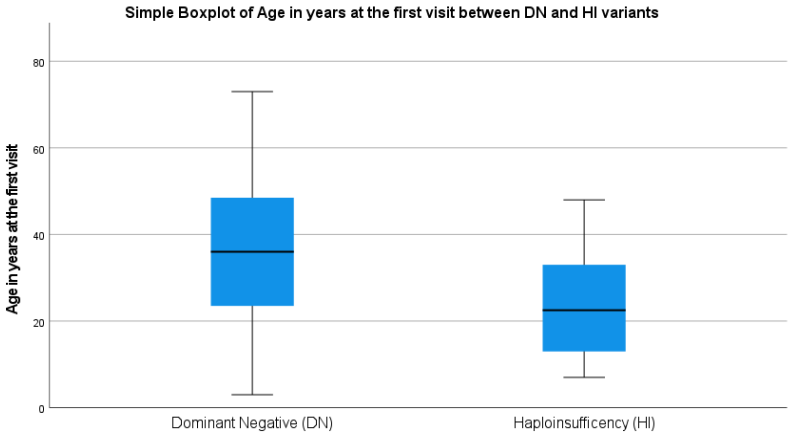

Figure 8. Boxplot of Age in years at the first visit between patients with DN and HI variants

In Table 25 demographic and clinical data are reported according to DN and HI variants. The prevalence of systemic score ≥7 and thoracic aortic surgery was higher even if they did not reach the statistical significance in HI that in DN patients.

Table 25. Population Data and Clinical manifestations between subjects with DN and HI variants.

	Patients (N=15) with DN variants	Patients (N=14) with HI variants	P value (Fisher's exact test)
Female Sex, n (%)	10 (66.7)	7 (50)	p = 0.458
Paediatric, n (%)	3 (20)	4 (28.6)	p = 0.297
Thumb Sign, n (%)	6 (40)	6 (42.8)	p = 0.587
Wrist Sign, n (%)	4 (26.6)	7 (50)	p = 0.181
Pectus Carinatum, n (%)	6 (40)	7 (50)	p = 0.434
Pectus Excavatum, n (%)	5 (33.3)	7 (50)	p = 0.297
Chest wall asymmetry, n (%)	2 (13.3)	3 (21.4)	p = 0.465
Hindfoot Valgus, n (%)	2 (13.3)	6 (42.8)	p = 0.086
Plain flat foot, n (%)	4 (26.6)	10 (71.4)	**p = 0.020**
Pneumothorax, n (%)	1 (6.66)	1 (7.14)	p = 0.741
Dural Ectasia, n (%)	3 (20)	4 (21.4)	p = 0.458
Scoliosis, n (%)	7 (46.6)	11 (78.5)	p = 0.082
Thoracolumbar kyphosis, n (%)	7 (46.6)	2 (14.2)	p = 0.068
Dolichocephaly, n (%)	4 (26.6)	10 (71.4)	**p = 0.020**
Downward slanting palpebral fissures, n (%)	3 (20)	2 (14.2)	p = 0.535
Enophthalmos, n (%)	1 (6.66)	2 (14.2)	p = 0.473
Retrognathia, n (%)	5 (33.3)	6 (42.8)	p = 0.593
Malar Hypoplasia, n (%)	1 (6.66)	-	p = 0.517
Skin Striae, n (%)	8 (53.3)	11 (78.5)	p = 0.150
Myopia ≥ 3 dioptres, n (%)	6 (40)	5 (35.7)	p = 0.558
MVP, n (%)	6 (40)	7 (50)	p = 0.434
Sprains or dislocations, n (%)	2 (13.3)	4 (28.6)	p = 0.291
Contractures, n (%)	1 (6.7)	3 (21.4)	p = 0.272
Systemic Score ≥ 7, n (%)	7 (46.6)	10 (71.4)	p = 0.165
Ectopia Lentis, n (%)	4 (26.6)	2 (14.2)	p = 0.361
Z-score >2, n (%)	11 (73.3)	10 (71.3)	p = 0.369
TAA surgery, n (%)	2 (13.3)	6 (42.8)	p = 0.086
Non-aortic vascular manifestations, n (%)	3 (20)	1 (7.14)	p = 0.362

Statistical test performed for categorical data was Fisher's exact test

In table 26, the evaluation of aortic root z-score and systemic score are reported, showing that patients carriers of Cys variants had higher values than patients with other missense variants.

Table 26. Differences in measurements between subjects with cysteine (Cys) missense variants and subjects with other missense variants

	Patients (N=6) With Cys variants	N valid values	Patients (N=8) With other missense variants	N valid values	P value
Z-Score Aortic Root	3.64 (2.83-4.12)	6	2.73 (1.24-4.31)	7	p = 0.366
Z-Score Aortic Root (only adults' patients)	3.64 (3.10-4.27)	4	2.99 (1.85-4.77)	6	p = 0.476
Systemic Score	7.5 (3.25-9)	6	3.5 (3-7.25)	8	p = 0.228
Height (cm)	176.5 (160.25-180.75)	6	180 (171.5-188.75)	8	p = 0.282
Weight (kg)	48 (38.25-57.25)	6	75 (61.25-86.5)	8	**p = 0.003**
BMI	16.35 (14.66-17.91)	6	22.25 (19.38-25.11)	8	**p = 0.003**
Age in years at the first visit	23.5 (12.75-42.25)	6	40.5 (31.75-48.75)	8	p = 0.142

Continuous variables are expressed as median (IQR); comparisons were performed by the independent samples Mann-Whitney U test.

As shown in Table 27, patients with cysteine missense variants have a higher prevalence of large part of the systemic features, z-score major criterium (>2), and ectopia lentis.

Table 27. Clinical manifestations between patients with cysteine missense variants and other missense variants

	Patients (N=6) with Cys variants	Patients (N=8) with other missense variants	P value (Fisher's exact test)
Thumb Sign, n (%)	3 (50)	1 (12.5)	p = 0.175
Wrist Sign, n (%)	4 (66.6)	2 (25)	p = 0.156
Pectus Carinatum, n (%)	2 (33.3)	3 (37.5)	p = 0.657
Pectus Excavatum, n (%)	4 (66.6)	1 (12.5)	p = 0.063
Chest wall asymmetry, n (%)	-	2 (25)	p = 0.380
Hindfoot Valgus, n (%)	-	1 (12.5)	p = 0.671
Plain flat foot, n (%)	1 (16.6)	2 (25)	p = 0.615
Pneumothorax, n (%)	-	1 (12.5)	p = 0.571
Dural Ectasia, n (%)	2 (33.3)	1 (12.5)	p = 0.385
Scoliosis, n (%)	3 (50)	3 (37.5)	p = 0.529
Thoracolumbar kyphosis, n (%)	2 (33.3)	4 (50)	p = 0.471
Dolichocephaly, n (%)	3 (50)	1 (12.5)	p = 0.175
Downward slanting palpebral fissures, n (%)	2 (33.3)	1 (12.5)	p = 0.385
Enophthalmos, n (%)	1 (16.6)	-	p = 0.429

Retrognathia, n (%)	3 (50)	2 (25)	p = 0.577
Malar Hypoplasia, n (%)	1 (16.6)	-	p = 0.429
Skin Striae, n (%)	2 (33.3)	5 (62.5)	p = 0.296
Myopia ≥ 3 dioptres, n (%)	3 (50)	2 (25)	p = 0.343
MVP, n (%)	4 (66.6)	2 (25)	p = 0.156
Systemic Score ≥ 7, n (%)	4 (66.6)	2 (25)	p = 0.156
Zscore >2, n (%)	6 (100)	5 (62.5)	p = 0.269
Ectopia Lentis, n (%)	2 (33.3)	1 (12.5)	p = 0.385
TAA surgery, n (%)	-	2 (25)	p = 0.308
Non-aortic cardiovascular manifestations, n (%)	3 (50)	-	p = 0.154
Female Sex, n (%)	1 (16.6)	4 (50)	p = 0.238
Paediatric, n (%)	2 (33.3)	1 (12.5)	p = 0.385
Sprains or dislocations, n (%)	-	1 (12.5)	p = 0.571
Contractures, n (%)	-	-	NA

Patients with Pathogenic or Likely Pathogenic variants in the TGFβ Pathway

Eight Likely Pathogenic (LP) or Pathogenic (P) variants falling in genes encoding for the TGFβ pathway were found in eight different index cases (Table 28), thus confirming the diagnosis of Loeys-Dietz syndrome (LDS). Among the 8 variants identified, n=7 (87.5%) fell in the *SMAD3* gene and n=1 (12.5%) fell in the *TGFB3* gene. Among *SMAD3* variants, n=5 (71.4%) are missense variants, n=1 (14.2%) led to the formation of a premature stop codon and n=1 (14.2%) was suggestive of splice site alteration, as it was located at +2 position from the end of the exon (P035, Table 28). The variant present in the *TGFB3* gene is synonymous; therefore, it does not alter the amino acid sequence of the protein. However, according to the main *in silico* predictors, it was suggested its contribution in the alteration of the splicing donor site (Delta score SpliceAI = 0.70) (P026, Table 28).

Table 28. LDS variants with ACMG classifications and applied criteria.

ID case study	SMAD3 chr position	HGVS nomenclature (Coding DNA)	HGVS nomenclature (Protein)	ACMG SMAD3	ACMG SMAD3 criteria	TGFB3 chr position	HGVS nomenclature (Coding DNA)	HGVS nomenclature (Protein)	ACMG TGFB3	ACMG TGFB3 criteria
P003	chr15:67479721:TC:AA	c.1028_1029delTCinsAA	p.(Phe343Ter)	Likely Pathogenic	PVS1 very strong, PM2 supporting				.	
P004	chr15:67473780:G:A	c.860G>A	p.(Arg287Gln)	Pathogenic	PP3 strong, PP5 strong, PM5 moderate, PM1 moderate, PM2 supporting				.	
P007	chr15:67479826:A:G	c.1133A>G	p.(Lys378Arg)	Likely Pathogenic	PP3 strong, PM2 moderate, PM1 moderate, PP2 supporting				.	
P008	chr15:67457264:C:T	c.238C>T	p.(Arg80Trp)	Likely Pathogenic	PP3 strong, PM1 moderate, PM5 moderate, PM2 supporting				.	
P010	chr15:67479811:G:A	c.1118G>A	p.(Arg373His)	Pathogenic	PP3 strong, PP5 strong, PM5 moderate, PM1 supporting, PM2 supporting				.	
P026						chr14:76427266:C:T	c.1080G>A	p.(Thr360=)	Likely Pathogenic	PP3 strong, PM2 supporting,

										PP5 supporting
P033	chr15:67479772:T:G	c.1079T>G	p.(Phe360Cys)	Likely Pathogenic	PP3 strong, PM1 supporting, PM2 supporting				.	
P035	chr15:67477204:T:C	c.1009+2T>C		Likely Pathogenic	PVS1 very strong, PM2 supporting				.	

HGVS (Human Genome Variation Society) nomenclature (https://hgvs-nomenclature.org/stable/)

In Table 29, data concerning vascular aortic and non-aortic manifestations in LDS patients are shown.

Table 29. Demographic and vascular manifestations in LDS patients

ID Case study	Sex	Age in years at the first visit	Aortic root diameters (mm)	Z-score aortic root	TAA surgery	Age in years at first TAA surgery	Non-aortic Vacular Manifestations	Age in years at first non-aortic vascular manifestations
P003	Male	45	.	.	Type A aortic dissection	39	Heart failure	46
P004	Male	60	37	.	elective surgery	56	Emorrhagic Stroke	65
P007	Female	31	36	2.22	.	.	spontaneous coronary artery dissection , Short-term cardiac arrest	31
P008	Male	62	.	.	Type A aortic dissection	62	Heart failure	NA
P010	Male	55	.	.	Type A aortic dissection	33	.	.
P026	Male	38	39	1.99	.	.	.	.
P033	Female	52	41	3.48	Type A aortic dissection	49	.	.
P035	Male	64	50	6.02	elective surgery	61	.	.

Given the rarity of the variants in the TGFB pathway, to make the analysis more meaningful and to observe how the variants segregated with the phenotype, we extended the analysis to the 21 available relatives of the index cases by Sanger sequencing, among whom 13 inherited the variant from the index case.

The c.238C>T (p.Arg80Trp) variant was identified at the heterozygous state in the exon 2 of the *SMAD3* gene in patient P008 (Male, 62 yrs at first visit, age death 71 yrs, Figure 10). This variant is described in dbSNP (rs750707381) but not identified in the general population, and in ClinVar in subjects with aneurysm-osteoarthritis syndrome and in subjects with familial thoracic aortic aneurysm/dissection with uncertain clinical significance. The variant falls in the MH1 domain of the *SMAD3* protein. The subject P008 underwent aortic dissection and displayed dilated cardiomyopathy, but what led him to death was heart failure. This variant has been transmitted to the two Proband's daughters, both showing dilated cardiomyopathy and Mitral Valve Prolapse (MVP) and Mitral Annular Disjunction (MAD).

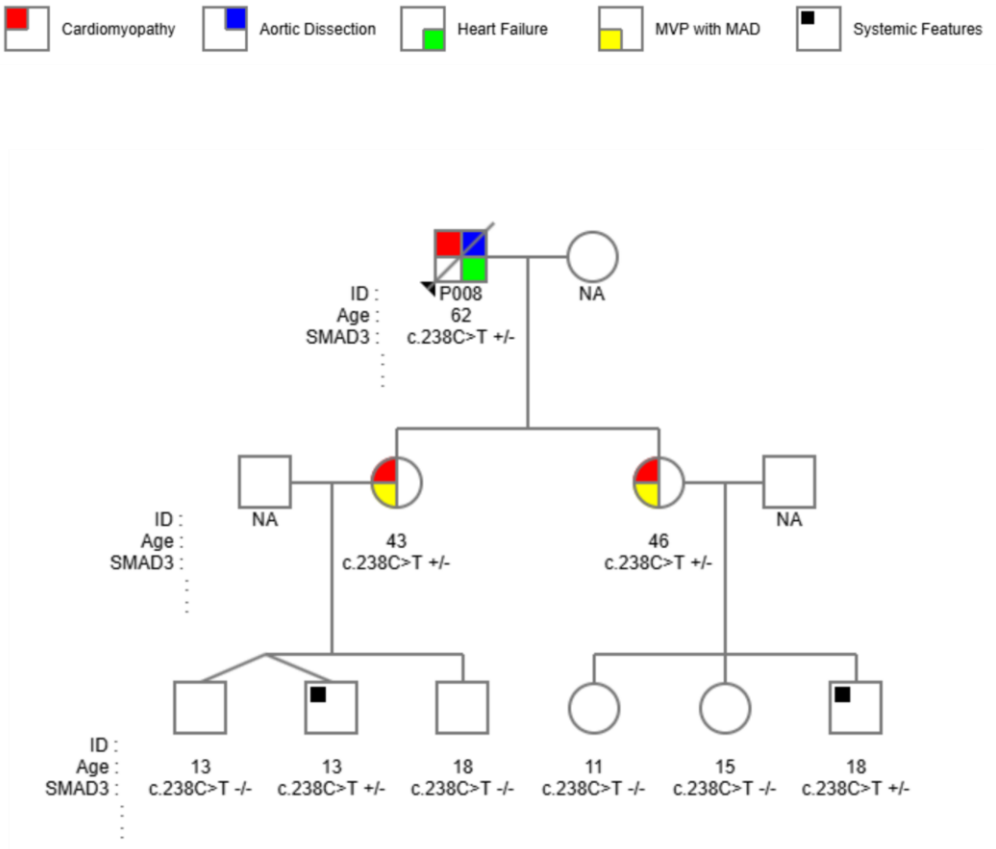

Figure 9. Pedigree patient P008

The c.860G>A (p.Arg287Gln) variant in exon 6 was identified at the heterozygous state in patient P004 (Male, 61 yrs at first visit, Figure 10). The variant is described in dbSNP (rs730880214) but not identified in the european population, and in ClinVar in subjects with Loeys-Dietz syndrome with uncertain clinical significance, in subjects with familial thoracic aortic aneurysm/dissection with likely pathogenic/pathogenic clinical significance and in subjects with aneurysm-osteoarthritis syndrome with likely pathogenic clinical significance. P004 had undergone open surgery for abdominal aortic aneurysm and ecstatic

ascending aorta replacement, and implantation of a biological prosthesis for insufficiency. He also exhibited periprosthetic aortic jet and mitral insufficiency secondary to mild-to-moderate valve prolapse. Moreover, P004 had a haemorrhagic stroke and underwent inguinal hernioplasty surgery.

The variant *SMAD3* c.860G>A was also present in Proband's sister, dead for type B aortic dissection, and in the children, with aortic root aneurysm (Figure 10).

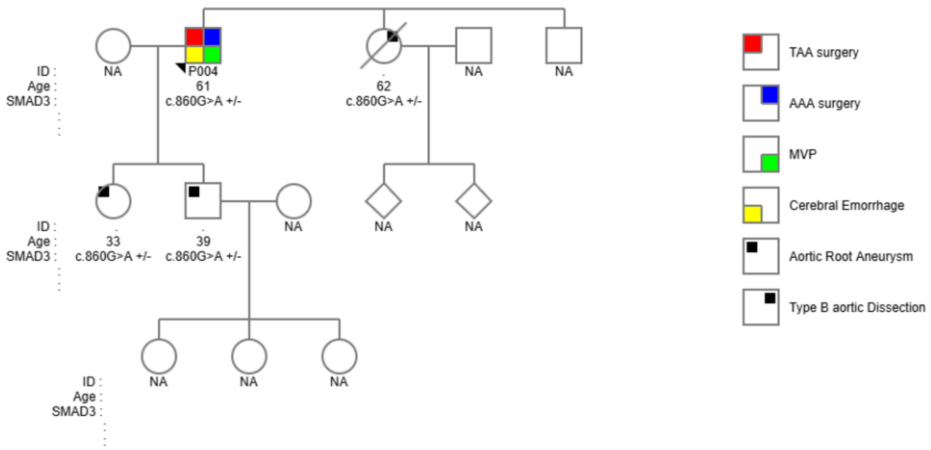

Figure 10. Pedigree patient P004

The variant c.1133A>G (p.Lys378Arg) was identified in exon 8, at the heterozygous state, in patient P007 (Female, 31 yrs at first visit, Figure 11). This variant is not reported in dbSNP and in gene and/or disease-specific databases and falls in the MH2 domain of SMAD3 protein, and it has been inherited from the father. Subject P007 experienced spontaneous coronary artery dissection following coronary angioplasty surgery; a short (1 minute) cardiac arrest was recorded during the procedure. Ascending aorta, aortic root and aortic arch are within normal limits (31, 36 and 24 mm, respectively). The aortic root Z-score for the patient P007 is 2.22.

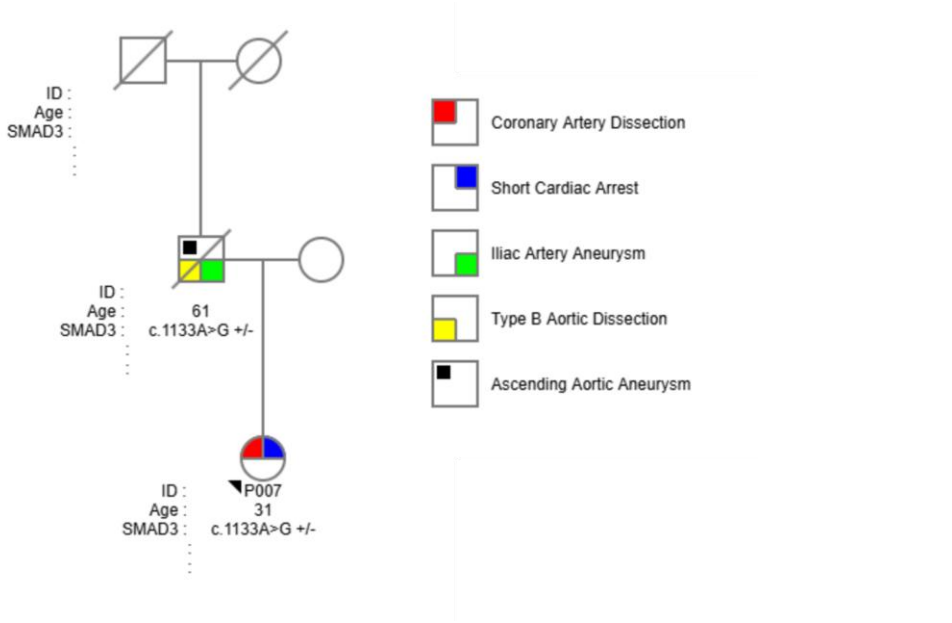

Figure 11. Pedigree of patient P007

The presence *in cis* of two missense variants [c.1028T>A (p.Phe343Tyr) and c.1029C>A (p.Phe343Leu)] in P003 subject (Male, 39 yrs at first visit, Figure 12), as confirmed by segregation analysis in family members, resulted in the introduction of a premature stop codon [c.1028_1029delTCinsAA (p.Phe343Ter)]. This variant is not reported in dbSNP or another database and has been transmitted to the son. Patient P003 presented an acute aortic dissection event (type A) with epiaortic vessel involvement, a picture complicated by acute thrombosis of the right coronary artery, ectasia of the celiac trunk, aneurysm of the proximal part of the 28 mm splenic artery and ectasia of the mesenteric artery. The patient P003 also displayed heart failure with reduced ejection fraction (FE 35-40%).

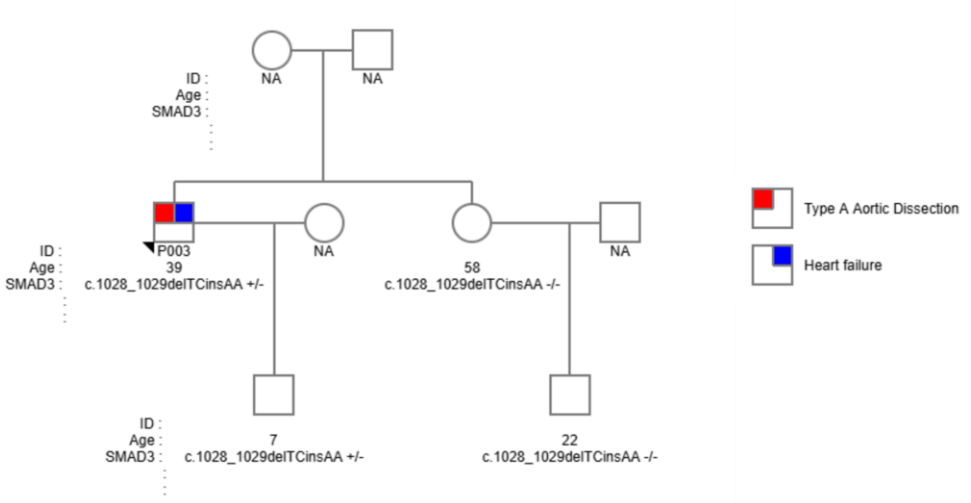

Figure 12. Pedigree of patient P003

The c.1009+2T>C variant was identified at the heterozygous state in intron 7 in the splicing consensus region in patient P035 (Male, 63 yrs at first visit, Figure 13) and was predicted to alter the splicing process by *in silico* tools. Subject P035 underwent mitral valvuloplasty surgery for a ruptured mitral chord presenting with aortic root ectasia (50 mm), aneurysmal dilatation of the right subclavian artery, aneurysms of the right bronchial and intercostal arteries, splenic artery and iliac arteries. This patient also underwent replacement of the ascending aorta. This variant, not reported in dbSNP and in gene and/or disease-specific databases, has been transmitted to the daughters, both showing mitral regurgitation and subclavian artery ectasia. One of them also reported the presence of MAD.

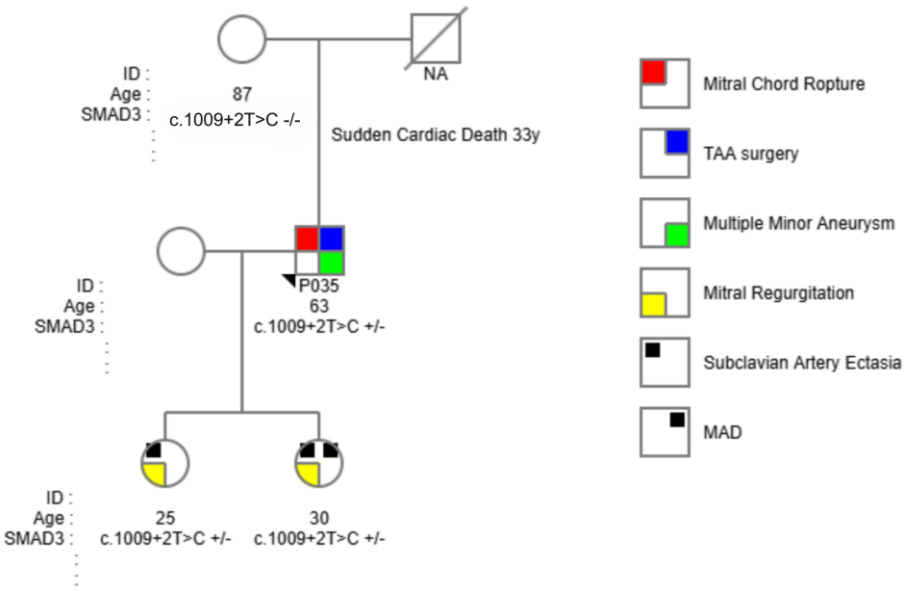

Figure 13. Pedigree of patient P035

The c.1079T>G (p.Phe360Cys) variant was identified at the heterozygous state in exon 8 of the *SMAD3* gene in patient P033 (Female, 52 yrs at first visit). It has not been reported in dbSNP and in gene and/or disease-specific databases. Patient P033 had no relatives (except for the brother, who resulted negative after testing for genetic analysis in a centre outside our own). Patient P033 underwent type A aortic dissection, and was treated throughout ascending aorta and aortic valve replacement. This patient also showed mitral prolapse of both leaflets with middle insufficiency, spinocellular carcinoma of the lower lip, myopia, scoliosis, previous bilateral cataract surgery, osteoporosis, sub-clinical hypothyroidism, chronic lower venous insufficiency with varices, fibromyalgia, and gastro-oesophageal reflux disease. At the last cardiological examination, she displayed aortic valved tube with a normalised mechanical prosthesis with normal trans prosthetic gradients (Gmax 10 mmHg), aortic arch of 27 mm at the emergence of epiaortic vessels, abdominal aorta of 42 mm, intimal flap visible.

The c.1118G>A p.(Arg373His) variant has been identified at the heterozygous state in exon 8 of the *SMAD3* gene in patient P010 (Male, 55 yrs at first visit). At 33 years of age, the patient underwent ascending aortic replacement with a valved conduit containing a mechanical prosthesis due to a Type A dissection. The most recent echocardiogram showed the results of aortic valve replacement, with a

normally positioned mechanical prosthesis. The ascending aorta measured 33 mm, and the aortic arch 26 mm. Redundancy of the subvalvular mitral apparatus with mild valvular insufficiency was also observed.

The c.1080G>A (p.Thr360=) variant has been found at the heterozygous state in exon 6 of the *TGFB3* gene in patient P026 (Male, 38 yrs at first visit, Figure 14). The variant is synonymous, so it does not alter the amino acid, but by falling on the last base of the exon, according to the main *in silico* prediction tools, it should lead to a splicing alteration (SpliceAI Donor Loss delta score = 0.70, dbscSNV Ada = Deleterious, CADD = 23.7). The subject P026 exhibited aortic root aneurysm (39 mm, z-score 1.99) and minimal systolic flattening of the mitral leaflets. As concerns systemic features, he had positive wrist and thumb signs. No other systemic abnormalities were reported. Segregation analysis in family members showed the identification of the variant in the mother, who displayed aortic root ectasia (38 mm, z-score of 1.8), and one of the two P026 sisters investigated (42 yrs), who did not present any aortic phenotype but underwent transcatheter supraventricular tachycardia (TPSV) ablation surgery.

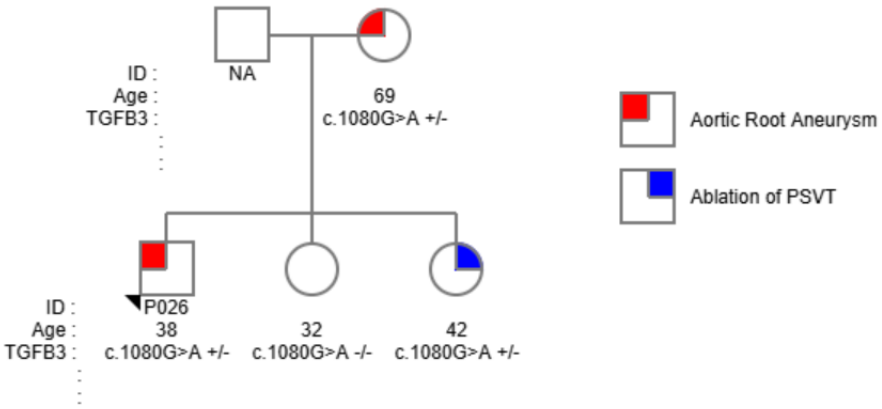

Figure 14. Pedigree of patient P026

Comparison between subjects with LP/P variants in the *FBN1* gene and subjects with variants in the TGFβ pathway genes

In table 30, data concerning differences in demographic and vascular parameters between patients with *FBN1* variants and patients with TGFβ pathway genes variants are reported. Patients carrying LP/P variants in TGFβ pathway genes showed higher age at the first visit and weight median values with respect to those with *FBN1* variants (Table 30).

Table 30. Differences in demographic and vascular parameters between patients with *FBN1* variants and patients with TGFβ pathway genes variants

	Patients (N=29) with FBN1 variants	N valid values	Patients (N=8) with TGFβ variants	N valid values	p value
Age in years at the first visit	27 (16-41.50)	29	53.5 (39.75-61.50)	8	**p= 0.004**
Height in cm	180 (173.5-185)	28	185 (175.75-196)	8	p= 0.267
Weight in kg	64 (55-78)	27	89.50 (71.50-99.25)	8	**p=0.008**
BMI	19.15 (17.28-24.62)	27	24.70 (21.50-27.21)	8	**p=0.017**
Systemic score	7 (4-9)	29	3.50 (2.25-7.00)	8	p=0.073
Aortic Root Z-score	3.64 (2.68-4.40)	25	2.22 (1.99-NA)	4	p=0.215
Age in years at time of TAA	41 (27.25-42.00)	8	52.50 (37.50-61.25)	6	p=0.108

Continuous variables are expressed as median (IQR); comparisons were performed by the independent samples Mann-Whitney U test.

Comparisons in age at the first visit and weight according to the presence of FBN1 variants or TGFβ pathway genes (LDS) variants are shown in Figure 15.

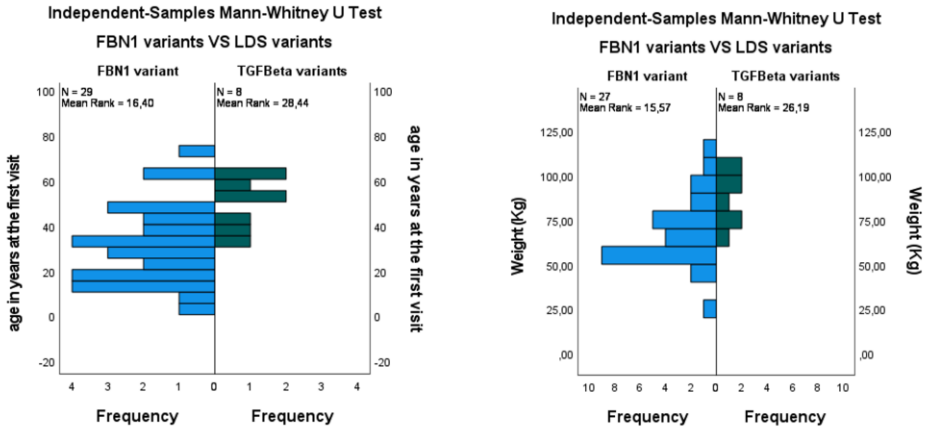

Figure 15. Independent Samples Mann-Whitney for age in years at the first and weight for patients with *FBN1* variants and patients with TGFβ pathway genes variants

In table 31 demographic and clinical characteristics between the two groups of patients are reported. Patients with *FBN1* variants shows a higher prevalence of skin striae and others systemic features, while patients with TGFβ variants have a higher prevalence of TAA surgery and non-aortic vascular manifestations.

Table 31. Clinical manifestation between patients with *FBN1* variant and patients with TGFβ variants

	Patients with FBN1 variants (N=29)	Patients with TGFβ variants (N=8)	p value
Male gender, n(%)	12 (41.4)	6 (75)	p=0.099
Paediatric Patients, n(%)	6 (20.6)	0	p=0.152
Thumb Sign, n (%)	12 (41.3)	3 (37.5)	p=0.588
Wrist Sign, n (%)	11 (37.9)	2 (25)	p=0.408
Pectus Carinatum, n (%)	13 (44.8)	4 (50)	p=0.553
Pectus Excavatum, n (%)	12 (41.3)	1 (12.5)	p=0.136
Chest wall asymmetry, n (%)	5 (17.2)	1 (12.5)	p=0.613
Hindfoot Valgus, n (%)	8 (27.5)	2 (25)	p=0.633
Plain flat foot, n (%)	14 (48.2)	3 (37.5)	p=0.447
Pneumothorax, n (%)	2 (6.9)	0	p=0.610
Dural Ectasia, n (%)	7 (24.1)	0	p=0.152
Scoliosis, n (%)	18 (62.0)	4 (50)	p=0.412
Thoracolumbar kyphosis, n (%)	9 (31.0)	3 (37.5)	p=0.520
Dolichocephaly, n (%)	14 (48.2)	4 (50)	p=0.621
Downward slanting palpebral fissures, n (%)	5 (17.2)	1 (12.5)	p=0.613
Enophthalmos, n (%)	3 (10.3)	1 (12.5)	p=0.640
Retrognathia, n (%)	11 (37.9)	2 (25)	p=0.648
Malar Hypoplasia, n (%)	1 (3.4)	0	p=0.784
Skin Striae, n (%)	19 (65.5)	2 (25)	p=**0.050**
Myopia ≥ 3 dioptres, n (%)	11 (37.9)	1 (12.5)	p=0.177
MVP, n (%)	13 (44.8)	3 (37.5)	p=0.517
Ectopia Lentis, n (%)	6 (27.5)	0	p=0.204
Systemic Score ≥ 7, n (%)	17 (58.6)	3 (37.5)	p=0.254
Dislocations, n(%)	6 (20.6)	0	p=0.204
Contractures, n(%)	4 (13.7)	1 (12.5)	p=0.708
Keloids, n(%)	2 (6.9)	0	p=0.610
TAA surgery, n (%)	8 (27.5)	6 (75)	p=**0.022**
Z score >2	21 (72.4)	3 (37.5)	p=0.553
Non-aortic vascular manifestations, n (%)	4 (13.7)	4 (50)	p=**0.049**

Statistical test performed is Fisher's Exact Test

In table 32 ocular manifestations between the two groups are reported. Patients with *FBN1* variants showed a slightly higher incidence of blue sclerae.

Table 32. Ocular clinical manifestations patients with *FBN1* variant and patients with TGFβ variants

	Patients with FBN1 variants (N=29)	Patients with TGFβ variants (N=8)	p value
Blue Sclerae, n(%)	9 (31)	2 (25)	p=0.556
Retina Leakage, n(%)	0	1 (12.5)	p=0.216
Glaucoma, n(%)	1 (3.4)	0	p=0.784
Cataract, n(%)	1 (3.4)	0	p=0.784

Statistical test performed is Fisher's Exact Test

In Figure 16 boxplot displaying the age (years) at the time of TAA surgery for the two groups (patients with *FBN1* variants or TGFβ variants), clustered by type of surgery (dissection or elective surgery) are reported. Patients carrying *FBN1* variants underwent elective surgery at a younger age than those who have dissection (p = 0.250). Conversely, in the TGFβ patients group, the median age at surgery for dissection is lower than that for elective surgery (p = 0.533). Patients carrying variants in TGFβ pathway genes (LDS) exhibited a higher median value of age at the time of elective surgery (Figure 16).

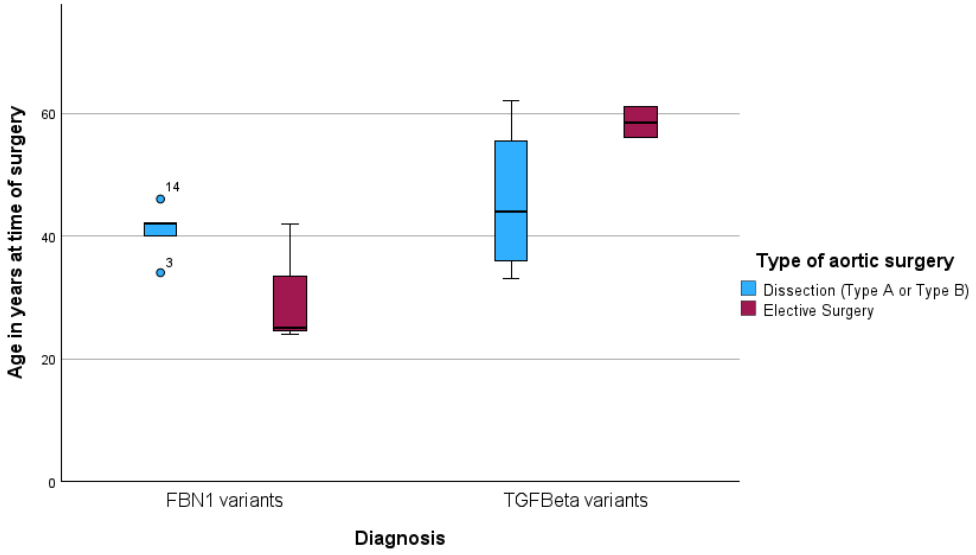

Figure 16. Boxplot of age in years at time of TAA Surgery

DISCUSSION

In PhD thesis the molecular characterisation of patients with Heritable Thoracic Aortic Disease (HTAD) - by establishing correlations between genotype and phenotype in patients who have suggestive variants classified as Likely Pathogenic or Pathogenic according to ACMG guidelines in the *FBN1* gene and the TGFβ pathway (including *TGFBR1*, *TGFBR2*, *SMAD2*, *SMAD3*, *TGFB2*, and *TGFB3* genes) - has been performed.

Among the whole cohort of 275 patients with aortic disease, the 37 subjects with aortopathy carrying LP/P variants in the selected genes (*FBN1* and TGFβ pathway genes) have some significantly different characteristics compared to the 238 patients without LP/P variants in the abovementioned genes. In particular, there is a higher prevalence of traditional cardiovascular risk factors (male gender, dyslipidemia, and even if not statistically significant hypertension and smoking habit). This datum is consistent with the presence in the group of 238 patients with aortopathy but without causative mutations in genes associated with diagnosis of Marfan syndrome, Loyes Dietz syndrome, isolated ectopia lentis and MASS of patients with a multifactorial aortopathy, due to the contribution of traditional cardiovascular factors to atherosclerotic pathogenesis (4). In fact, in the group of 238 are included patients with mutations in other genes associated with non-syndromic thoracic aortic aneurysm or without causative variants identified. Moreover, the 238 patients are characterized by a prevalent involvement of thoracic ascending aorta often related to a multifactorial burden of traditional cardiovascular factors and characterized by a strong inflammatory component (92).

According to previous literature data the 37 patients, prevalently diagnosed with a syndromic disorder (35/37 MFS and LDS) and with mutation in *FBN1* and TGFβ pathway genes, showed a reduced age at the first visit and a higher rate of thoracic aortic surgery (4).

Several data from literature demonstrated that thoracic aortic aneurysm and acute aortic dissection are more common in male patients, representing about two-thirds of cases in large registries. Female patients tend to present about a decade later and show faster aneurysm growth rates, but prevalence remains higher in men overall (93). The main genetic pathogenesis due to causative rare variants of MFS and LDS and the autosomal dominant inheritance leads to a equal involvement of males and females (94–96). Both LDS and MFS patients experience TAA surgery at a younger age and have a higher rate of aortic surgery due to the aggressive nature of their aortopathies and the early onset of complications.

This work also aimed to assess how causative variants of the *FBN1* gene influence patients' phenotypes, both at the cardiovascular and systemic levels. Of the 29 subjects with mutations in *FBN1*, 27 were diagnosed with Marfan syndrome, one subject with MASS phenotype [c.409C>T p.(Gln137Ter), P031] and one subject with Ectopia Lentis [c.5592_5594dup p.(Gln1864_Cys1865insTrp), P018]. While *FBN1* gene mutations are consistently associated with isolated ectopia lentis, no previously published case report was found that describes an *FBN1* in-frame duplication associated with isolated ectopia lentis. There are no studies on large patient series reporting a specific

correlation between MASS phenotype and haploinsufficiency variants. However, a case report by Carmela Fusco et al. describes a subject with MASS syndrome with a truncated variant, caused by the retention of intronic nucleotides, which led to the introduction of a premature stop codon (97).

Among our LP/P *FBN1* patients, we observe that individuals with mutations determining the introduction of a premature stop codon or a defect in the mRNA maturation process potentially associated with haploinsufficiency (HI) variants have a lower age at first visit compared to those with dominant negative (DN) variants. Our data are in keeping with those of Takeda et al. (98).

Furthermore, in our population, the median systemic score and the prevalence of patients exceeding the systemic score cutoff of 7 points representing a major criterium in the Ghent nosology (12) are higher in patients with HI variants compared to those with DN variants. Consistently with our data, in a paediatric cohort study reported at the ESC Congress 2021, patients with nonsense/frameshift variants (classified as Haploinsufficiency (HI) variants), exhibited the highest rate (44.8%) of positive systemic scores (score >= 7) (99) with respect to the patients with DN variants.

We reported a significant difference for plain flat foot and dolichocephaly, both more present in patients with HI variants. The current literature about genotype-phenotype correlations in patients with *FBN1* LP/P variants does not offer specific statistical data to support those observations directly, but regarding the plain flat foot, some authors report that Haploinsufficiency (HI) mutations are consistently linked to a more severely affected skeletal phenotype (100,101).

A difference in weight is observed between subjects with cysteine missense variants and subjects with other missense variants, as well as BMI (Body Mass Index). There aren't any similar observations reported in the literature, but according to a study, mutations in the *FBN1* gene can be associated with depleted or abnormal adipose tissue, a feature observed in some patients with Marfan syndrome and lipodystrophies (102). In their work about the expression of *FBN1* during adipogenesis, they found that *FBN1* mRNA was up-regulated in the adipose tissue of obese women compared to non-obese women, and associated with an increase in adipocyte size. These results are consistent with the finding of reduced subcutaneous tissue with abnormal adipocytes in some Marfan syndrome patients (103). Therefore, downregulation of *FBN1* following a missense variant in cysteine may affect weight and BMI in a more severe manner with respect to other missense variants.

HI patients in our study showed a more severe systemic and vascular phenotype and among patients with missense mutations those with cysteine substitution showed a worse phenotype. Studies on larger cohorts are present in the literature, showing that patients with HI variants or DN variants involving cysteine residues should be monitored more closely, as these patients are more prone to rapid develop aortic root aneurysms/dissections (97, 98).

Based on the existing knowledge, patients with truncating variants in *FBN1* (which include nonsense or frameshift) exhibit a higher proportion of aortic events (such as prophylactic surgery for aneurysm or dissection) compared to those with missense mutations. In the study of Franken R et al., MFS patients with

an HI-*FBN1* mutation showed a 2.4-fold increased risk for the combined clinical endpoint of aortic dissection and cardiovascular death in comparison with MFS patients with a DN-*FBN1* mutation (100). In a Japanese cohort analysed by Takeda at al., the risk of severe aortic events was significantly higher in the HI group than in the DN group (98). The evidence that in our analysis the higher prevalence of TAA surgery in HI patients in comparison with DN patients did not reach the statistical significance may be due to the relatively small dataset size of our population.

The data presented in this thesis concerning TGFbeta pathway genes, allowing us to diagnose 8 LDS patients, offer insights into the correlation between *SMAD3* genotype and phenotype. As concerns cardiovascular manifestations, 6 out of the 7 patients with *SMAD3* variants underwent thoracic aortic surgery at a mean age of 51.5 years; the subject not undergoing surgery was the youngest (33 years) and had an aortic root aneurysm of 36 mm in close follow-up for progression. Interestingly, four out of the 7 *SMAD3* patients also showed non-aortic vascular phenotypes: 2 patients (P008 and P003) had heart failure, which in one case (P008) led to death; one had a brief cardiac arrest as a consequence of coronary dissection (P007), and the fourth had an episode of haemorrhagic stroke (P004).

Concerning the 8 LDS index cases with causative variants in *SMAD3* (n=7) or *TGFB3* (n=1), for 6 patients first degree family members were available for segregation analysis.

As concerns P008 subject, in whom a mutation in the MH1 domain of SMAD3 protein was identified (c.238C>T, p.Arg80Trp), he showed dilated cardiomyopathy determining heart failure and in turn death. Previous data from the literature showed that this variant was previously observed in a subject with aortic dilatation (104). Interestingly, the genetic variant identified in the P008 subject is located in the MH1 domain, in which no variants have been previously described in association with non-aortic phenotype. Actually, previous data from literature consistently reported the involvement of haploinsufficiency or missense dominant negative variants located in the SMAD3 MH2 domain in patients also showing heart failure and/or cardiomyopathy (61). The variant identified in the proband was also present in the two daughters, who showed mitral valve prolapse with mitral annular disjunction (MAD) associated with dilated cardiomyopathy, as the father, thus supporting the evidence of segregation of the cardiac phenotype across generations. This variant was also inherited by the proband's grandchildren, on whom it is not possible to further speculate due to their young age. Moreover, P003 patients carrying a haploinsufficiency variant [c.1028_1029delTCinsAA (p.Phe343Ter)] also presented heart failure at the age of 45 years. A clinical follow-up evaluation of the P003 subject also reported an episode of sustained ventricular tachycardia treated with shock and subsequent cardioversion, as well as atrial fibrillation events.

The observation of a potential association of *SMAD3* variants also with atrial fibrillation is supported by data from the literature, showing the presence of ventricular tachycardia episodes in subjects carrying *SMAD3* pathogenic mutations (61,62). Moreover, an international retrospective cohort study reported the presence of the phenotypes mentioned above in subjects carrying pathogenic variants in genes encoding fibrillin 1 and TGF-β signalling members,

compared to subjects carrying genetic variants in the *ACTA2* gene (60).

The P004 patient, carrying the c.860G>A (p.Arg287Gln) variant [previously reported in literature in association to *SMAD3*-related conditions (39,64,105,106)] had a hemorrhagic stroke at the age of 66 years with minimal outcomes in the right upper hemisoma, so determining worsening asthenia and the appearance of pain in the right shoulder and loss of strength in the right leg. Actually, in a study by Silvy Dekker et al. (107), aiming at reporting neurovascular findings in patients with Loeys Dietz syndrome type III, neurovascular imaging showed abnormalities such as aneurysm, tortuosity, coiling and kinking in the vast majority of patients; anyway, no cerebrovascular haemorrhage or ischemic stroke occurred. A further study revealed the occurrence of TIA (transient ischemic attack) in a patient with a pathogenic *SMAD3* variant (108). Data from the present study might support previously reported information concerning the presence of neurovascular manifestations in LDS type III patients.

Patient P007 was admitted to the hospital for chest pain with anterior ST-segment elevation. Angiographic examination showed spontaneous coronary artery dissection (SCAD). During the procedure, she also experienced a short cardiac arrest (1 minute). This phenotype has been reported in other studies in subjects with *SMAD3* mutations (64,109); interestingly, in the P007 patient, as well as in case reports from the literature with Spontaneous Coronary Artery Dissection (SCAD), the affected patients are young women with a strong smoking habit.

In our cohort of subjects with *SMAD3* pathogenic or likely pathogenic variants, mitral valve disorders are the most frequently reported manifestation; among 18 subjects with pathogenic variants in *SMAD3* gene (7 index cases and 11 first-degree relatives), seven subjects had mitral valve prolapse (MVP). Moreover, P035 subject had valvuloplasty surgery for ruptured mitral chord and one of his daughter showed flattening of the mitral leaflets. Of the 7 subjects with MVP, 3 also had mitral annular disjunction (MAD). A recent study on the Montalcino Aortic Consortium showed an enrichment in *SMAD3* pathogenic variants in patients with MAD, with respect to other genes encoding different components of the TGFβ signalling pathway; moreover, Mitral Valve Prolapse was observed in 20% of the population with *SMAD3* pathogenic variants (110). Data from the present study support previously suggested evidence of a contribution of *SMAD3* genetic variants to phenotypic manifestations associated with LDS type III, ranging from aortopathy to non-aortic vascular phenotypes, which, even if more rarely, should not be underestimated.

One patient in our LDS cohort has a likely pathogenic variant in the *TGFB3* gene: he carried a c.1080G>A variant, a synonymous variant p.(Thr360=) that all *in silico* predictors strongly suggested to alter splicing mechanism. To date no functional analyses to verify the effect of the variant on mRNA maturation process are available. The subject inherited the variant from his mother. Both index case and his mother have mild aortic root ectasia. It is interesting to note that the older sister also carrier of the same mutation does not have an aortic phenotype but underwent transcatheter supraventricular tachycardia (TPSV) ablation surgery.

A limit of the present work in LDS patient molecular characterization is the lack of information concerning genetic variants in other genes beyond those

investigated possibly contributing to further non-aortic phenotypes (i.e. cardiomyopathy). Nevertheless, in order to exclude the contribution of further variants in influencing clinical manifestations in more complex phenotypes, whole exome sequencing analysis (WES) is currently being carried out.

In our case series of subjects with LP/P variants in *FBN1* gene and genes associated with LDS, a significant difference in age at diagnosis was present with a significantly lower age in subjects carrying *FBN1* variants than in those with TGFβ pathway variants. This observation is supported in the literature by a recent study comparing patients with variants in *FBN1* and patients with variants in the *SMAD3* gene. Calderon-Martinez et al. found that the median age for patients with *FBN1* pathogenic variants was 30.7 years (IQR 17.5-45.2), with respect to the median age of *SMAD3* pathogenic variants patients of 45 years (IQR 27-58.2) (111). Other studies did not show significant differences concerning median age between similar groups. Yagyu et al. reported that the median age at heritable thoracic aortic disease (HTAD) diagnosis was 34.0 years for patients in Group 1 (*FBN1* variants) and 34.0 years for patients in Group 2 (*TGFBR1*, *TGFBR2*. *SMAD3*, or *TGFB2* variants) (112). Mühlstädt et al. found that the mean age at initial contact was 34 ± 18 years for both the Marfan syndrome group (*FBN1*) and the Loeys-Dietz syndrome group (including *TGFBR1*, *TGFBR2*, and *SMAD3*) (113). This discrepancy could be due to two factors: 1) the study that highlights a significant difference involved the largest number of subjects thus allowing a strong statistical power (1.780 patients: 1.028 with *FBN1* variants and 196 with *SMAD3* variants); 2) the comparison is made individually at the level of the various genes that fall within the TGFβ pathway, while in the two studies that do not show significant age differences, the TGFB pathway genes are grouped.

In our study, subjects with LP/P variant associated with LDS have a higher rate of thoracic aortic surgery (defined as the sum of elective surgery and acute dissection) than subjects with LP/P variants in *FBN1*. This observation is consistent with that by Calderon-Martinez et al., who defined "aortic events" as aortic dissections, ruptures or aneurysms requiring surgical repair, and showed that the prevalence of aortic events was 33.7% for *SMAD3* (66 out of 196 patients) and 22.9% for *FBN1* (236 out of 1028 patients) (111).

In our case series, non-aortic vascular events (heart failure, stroke, NSTEMI, carotid dissection, cardiac arrest, and cardioversion) were more frequent in subjects with LP/P variants in the TGFB pathway than in subjects with LP/P variants in *FBN1*. Direct, large-scale studies that specifically compare the prevalence of non-aortic cardiovascular outcomes between patients with *FBN1* and *SMAD3* pathogenic variants are limited. The available literature primarily consists of case reports and small studies that focus on the vascular manifestations of each syndrome. There is only one international retrospective study that focuses on similar phenotypes on HTAD. The Authors concluded that in patients with HTAD, arrhythmia and impaired myocardial function were found in patients harbouring LP/P variants in the *FBN1* gene and TGF-β signalling genes, but not in patients carrying LP/P variants in the *ACTA2* gene. Nevertheless, breaking down the data for the TGF-β pathway shows that the gene in which there are more non-aortic vascular phenotypes is *SMAD3* (60).

Another significant observation in our population concerns skin striae, which are significantly more prevalent in individuals with *FBN1* LP/P variants than in those

with TGFβ LP/P variants. Lindsay. M. E. et al. in a study published in 2012, noted that while skin striae can be a shared feature between Marfan and Loeys-Dietz syndromes, they are more strongly associated with the Marfan phenotype (46). Even in the foundational paper that first described Loeys-Dietz syndrome, in the clinical description of the patients, the Authors explicitly note some differences in LDS patients from the classic Marfan syndrome phenotype “skin striae”(40).

Concerning aortic surgery (elective surgery or dissection), in subjects with MFS, the median age for elective surgery is lower than that for dissection, while in LDS subjects the median age at the time of dissection is lower than the median age at elective surgery. Due to better defined clinical criteria and clinical management for Marfan syndrome and the more evident systemic phenotypes allowing a earlier diagnosis, subjects with Marfan syndrome receive better aortic prophylaxis with respect to LDS patients. Individuals with LDS syndrome undergo a more complicated diagnostic process, which often is achieved after the occurrence of vascular events (aortic or non-aortic).

CONCLUSIONS

This thesis supports the concept that *SMAD3* variants might be associated with a variable spectrum of clinical manifestations, with inter- and intra-familial variability in their phenotypic expression. In particular, the present work supports the relationship between *SMAD3* variants and the occurrence of non-aortic phenotypes, beyond vascular manifestations widely described in Loeys-Dietz patients. Moreover, genetic data also showed the possible contribution of aminoacidic alteration of a further protein domain (MH1), beyond MH2, in determining non-aortic manifestations.

The comparison of clinical manifestations between subjects with *FBN1* variants and those with TGFβ pathway genes (related to LDS) variants confirms a more severe aortic phenotype in LDS patients, also showing a higher dissection rate, and highlights a higher prevalence of non-aortic manifestations in these patients. Moreover, LDS patients showed a delayed age at diagnosis as well as a delayed age at elective surgery, with respect to *FBN1* carriers. This issue underlines the need of an earlier multidisciplinary diagnostic assessment, also including genetic evaluation, in these subjects, who often undergo a more complicated diagnostic process, achieved after the occurrence of vascular events (aortic or non-aortic).

Further functional studies and enrolment of larger cohorts might be useful in order to deepen the molecular mechanisms underlying genotype-phenotype correlations. Moreover, results from more detailed analyses [i.e. whole exome sequencing (WES) approach] in subjects with a more complex phenotype may be useful in order to exclude the contribution of further variants.

BIBLIOGRAPHY

1. Zhou Z, Cecchi AC, Prakash SK, Milewicz DM. Risk Factors for Thoracic Aortic Dissection. Genes. 7 ottobre 2022;13(10):1814.

2. Howard DPJ, Banerjee A, Fairhead JF, Perkins J, Silver LE, Rothwell PM, et al. Population-based study of incidence and outcome of acute aortic dissection and premorbid risk factor control: 10-year results from the Oxford Vascular Study. Circulation. 21 maggio 2013;127(20):2031–7.

3. Tanaka Y, Sakata K, Sakurai Y, Yoshimuta T, Morishita Y, Nara S, et al. Prevalence of Type A Acute Aortic Dissection in Patients With Out-Of-Hospital Cardiopulmonary Arrest. Am J Cardiol. 1 giugno 2016;117(11):1826–30.

4. Isselbacher EM, Preventza O, Hamilton Black J, Augoustides JG, Beck AW, Bolen MA, et al. 2022 ACC/AHA Guideline for the Diagnosis and Management of Aortic Disease: A Report of the American Heart Association/American College of Cardiology Joint Committee on Clinical Practice Guidelines. Circulation [Internet]. 13 dicembre 2022 [citato 14 maggio 2025];146(24). Disponibile su: https://www.ahajournals.org/doi/10.1161/CIR.0000000000001106

5. De Cario R, Giannini M, Cassioli G, Kura A, Gori AM, Marcucci R, et al. Tracking an Elusive Killer: State of the Art of Molecular-Genetic Knowledge and Laboratory Role in Diagnosis and Risk Stratification of Thoracic Aortic Aneurysm and Dissection. Diagnostics. 22 luglio 2022;12(8):1785.

6. Cecchi AC, Drake M, Campos C, Howitt J, Medina J, Damrauer SM, et al. Current state and future directions of genomic medicine in aortic dissection: A path to prevention and personalized care. Semin Vasc Surg. marzo 2022;35(1):51–9.

7. Maleszewski JJ, Miller DV, Lu J, Dietz HC, Halushka MK. Histopathologic findings in ascending aortas from individuals with Loeys-Dietz syndrome (LDS). Am J Surg Pathol. febbraio 2009;33(2):194–201.

8. Franken R, den Hartog AW, de Waard V, Engele L, Radonic T, Lutter R, et al. Circulating transforming growth factor-β as a prognostic biomarker in Marfan syndrome. Int J Cardiol. 3 ottobre 2013;168(3):2441–6.

9. Chiu HH, Wu MH, Chen HC, Kao FY, Huang SK. Epidemiological profile of Marfan syndrome in a general population: a national database study. Mayo Clin Proc. gennaio 2014;89(1):34–42.

10. Dietz HC, Cutting GR, Pyeritz RE, Maslen CL, Sakai LY, Corson GM, et al. Marfan syndrome caused by a recurrent de novo missense mutation in the fibrillin gene. Nature. 25 luglio 1991;352(6333):337–9.

11. Ramirez F, Rifkin DB. Cell signaling events: a view from the matrix. Matrix Biol. aprile 2003;22(2):101–7.

12. Loeys BL, Dietz HC, Braverman AC, Callewaert BL, De Backer J, Devereux

RB, et al. The revised Ghent nosology for the Marfan syndrome. J Med Genet. luglio 2010;47(7):476–85.

13. Sheikhzadeh S, Kade C, Keyser B, Stuhrmann M, Arslan-Kirchner M, Rybczynski M, et al. Analysis of phenotype and genotype information for the diagnosis of Marfan syndrome. Clin Genet. settembre 2012;82(3):240–7.

14. Milewicz DM, Braverman AC, De Backer J, Morris SA, Boileau C, Maumenee IH, et al. Marfan syndrome. Nat Rev Dis Primers. 2 settembre 2021;7(1):64.

15. Sadiq MA, and Vanderveen D. Genetics of Ectopia Lentis. Seminars in Ophthalmology. 1 settembre 2013;28(5–6):313–20.

16. Silverman DI, Burton KJ, Gray J, Bosner MS, Kouchoukos NT, Roman MJ, et al. Life expectancy in the Marfan syndrome. Am J Cardiol. 15 gennaio 1995;75(2):157–60.

17. Jondeau G, Detaint D, Tubach F, Arnoult F, Milleron O, Raoux F, et al. Aortic event rate in the Marfan population: a cohort study. Circulation. 17 gennaio 2012;125(2):226–32.

18. Roman MJ, Rosen SE, Kramer-Fox R, Devereux RB. Prognostic significance of the pattern of aortic root dilation in the Marfan syndrome. J Am Coll Cardiol. 1 novembre 1993;22(5):1470–6.

19. Prakash SK, Haden-Pinneri K, Milewicz DM. Susceptibility to acute thoracic aortic dissections in patients dying outside the hospital: an autopsy study. Am Heart J. settembre 2011;162(3):474–9.

20. Arnaud P, Milleron O, Hanna N, Ropers J, Ould Ouali N, Affoune A, et al. Clinical relevance of genotype-phenotype correlations beyond vascular events in a cohort study of 1500 Marfan syndrome patients with FBN1 pathogenic variants. Genet Med. luglio 2021;23(7):1296–304.

21. Hascoet S, Edouard T, Plaisancie J, Arnoult F, Milleron O, Stheneur C, et al. Incidence of cardiovascular events and risk markers in a prospective study of children diagnosed with Marfan syndrome. Arch Cardiovasc Dis. gennaio 2020;113(1):40–9.

22. Aydin A, Adsay BA, Sheikhzadeh S, Keyser B, Rybczynski M, Sondermann C, et al. Observational cohort study of ventricular arrhythmia in adults with Marfan syndrome caused by FBN1 mutations. PLoS One. 2013;8(12):e81281.

23. Hoffmann BA, Rybczynski M, Rostock T, Servatius H, Drewitz I, Steven D, et al. Prospective risk stratification of sudden cardiac death in Marfan's syndrome. Int J Cardiol. 10 settembre 2013;167(6):2539–45.

24. Pyeritz RE. Marfan syndrome: improved clinical history results in expanded natural history. Genet Med. agosto 2019;21(8):1683–90.

25. Faivre L, Collod-Beroud G, Loeys BL, Child A, Binquet C, Gautier E, et al. Effect of mutation type and location on clinical outcome in 1,013 probands with Marfan syndrome or related phenotypes and FBN1 mutations: an international

study. Am J Hum Genet. settembre 2007;81(3):454–66.

26. Turner CLS, Emery H, Collins AL, Howarth RJ, Yearwood CM, Cross E, et al. Detection of 53 FBN1 mutations (41 novel and 12 recurrent) and genotype-phenotype correlations in 113 unrelated probands referred with Marfan syndrome, or a related fibrillinopathy. Am J Med Genet A. febbraio 2009;149A(2):161–70.

27. Kielty CM, Baldock C, Lee D, Rock MJ, Ashworth JL, Shuttleworth CA. Fibrillin: from microfibril assembly to biomechanical function. Philos Trans R Soc Lond B Biol Sci. 28 febbraio 2002;357(1418):207–17.

28. Judge DP, Biery NJ, Keene DR, Geubtner J, Myers L, Huso DL, et al. Evidence for a critical contribution of haploinsufficiency in the complex pathogenesis of Marfan syndrome. J Clin Invest. luglio 2004;114(2):172–81.

29. Neptune ER, Frischmeyer PA, Arking DE, Myers L, Bunton TE, Gayraud B, et al. Dysregulation of TGF-beta activation contributes to pathogenesis in Marfan syndrome. Nat Genet. marzo 2003;33(3):407–11.

30. Forteza A, Evangelista A, Sánchez V, Teixidó-Turà G, Sanz P, Gutiérrez L, et al. Efficacy of losartan vs. atenolol for the prevention of aortic dilation in Marfan syndrome: a randomized clinical trial. Eur Heart J. 21 marzo 2016;37(12):978–85.

31. Sandor GGS, Alghamdi MH, Raffin LA, Potts MT, Williams LD, Potts JE, et al. A randomized, double blind pilot study to assess the effects of losartan vs. atenolol on the biophysical properties of the aorta in patients with Marfan and Loeys-Dietz syndromes. Int J Cardiol. 20 gennaio 2015;179:470–5.

32. Anderson NK, Juzwiak EE, Dietz HC. A seX(X/Y) Article on Marfan Syndrome. J Am Heart Assoc. 20 ottobre 2020;9(20):e018814.

33. Overwater E, Efrat R, Barge-Schaapveld DQCM, Lakeman P, Weiss MM, Maugeri A, et al. Autosomal dominant Marfan syndrome caused by a previously reported recessive FBN1 variant. Mol Genet Genomic Med. febbraio 2019;7(2):e00518.

34. Eldadah ZA, Brenn T, Furthmayr H, Dietz HC. Expression of a mutant human fibrillin allele upon a normal human or murine genetic background recapitulates a Marfan cellular phenotype. J Clin Invest. febbraio 1995;95(2):874–80.

35. Loeys B. The search for genotype/phenotype correlation in Marfan syndrome: to be or not to be? Eur Heart J. 14 novembre 2016;37(43):3291–3.

36. Faivre L, Masurel-Paulet A, Collod-Béroud G, Callewaert BL, Child AH, Stheneur C, et al. Clinical and molecular study of 320 children with Marfan syndrome and related type I fibrillinopathies in a series of 1009 probands with pathogenic FBN1 mutations. Pediatrics. gennaio 2009;123(1):391–8.

37. Gao L, Tian T, Zhou X, Fan L, Wang R, Wu H. Detection of ten novel FBN1 mutations in Chinese patients with typical or incomplete Marfan syndrome and an overview of the genotype-phenotype correlations. Int J Cardiol. 15 ottobre 2019;293:186–91.

38. Pees C, Michel-Behnke I, Hagl M, Laccone F. Detection of 15 novel mutations in 52 children from 40 families with the Marfan or Loeys-Dietz syndrome and phenotype-genotype correlations. Clin Genet. dicembre 2014;86(6):552–7.

39. Schepers D, Tortora G, Morisaki H, MacCarrick G, Lindsay M, Liang D, et al. A mutation update on the LDS-associated genes TGFB2/3 and SMAD2/3. Human Mutation. 2018;39(5):621–34.

40. Loeys BL, Schwarze U, Holm T, Callewaert BL, Thomas GH, Pannu H, et al. Aneurysm syndromes caused by mutations in the TGF-β receptor. New England Journal of Medicine. 2006;355(8):788–98.

41. Loeys BL, Chen J, Neptune ER, Judge DP, Podowski M, Holm T, et al. A syndrome of altered cardiovascular, craniofacial, neurocognitive and skeletal development caused by mutations in TGFBR1 or TGFBR2. Nat Genet. marzo 2005;37(3):275–81.

42. van de Laar IMBH, Oldenburg RA, Pals G, Roos-Hesselink JW, de Graaf BM, Verhagen JMA, et al. Mutations in SMAD3 cause a syndromic form of aortic aneurysms and dissections with early-onset osteoarthritis. Nat Genet. febbraio 2011;43(2):121–6.

43. Regalado ES, Guo DC, Villamizar C, Avidan N, Gilchrist D, McGillivray B, et al. Exome sequencing identifies SMAD3 mutations as a cause of familial thoracic aortic aneurysm and dissection with intracranial and other arterial aneurysms. Circ Res. 2 settembre 2011;109(6):680–6.

44. Nevidomskyte D, Shalhub S, Aldea GS, Byers PH, Schwarze U, Murray ML, et al. Endovascular Repair of Internal Mammary Artery Aneurysms in 2 Sisters with SMAD3 Mutation. Ann Vasc Surg. maggio 2017;41:283.e5-283.e9.

45. Mégarbané A, Hanna N, Chouery E, Jalkh N, Mehawej C, Boileau C. Marfanoid habitus, inguinal hernia, advanced bone age, and distinctive facial features: a new collagenopathy? Am J Med Genet A. maggio 2012;158A(5):1185–9.

46. Lindsay ME, Schepers D, Bolar NA, Doyle JJ, Gallo E, Fert-Bober J, et al. Loss-of-function mutations in TGFB2 cause a syndromic presentation of thoracic aortic aneurysm. Nat Genet. 8 luglio 2012;44(8):922–7.

47. Gouda P, Kay R, Habib M, Aziz A, Aziza E, Welsh R. Clinical features and complications of Loeys-Dietz syndrome: A systematic review. International Journal of Cardiology. 1 settembre 2022;362:158–67.

48. Granadillo JL, Chung WK, Hecht L, Corsten-Janssen N, Wegner D, Nij Bijvank SWA, et al. Variable cardiovascular phenotypes associated with SMAD2 pathogenic variants. Hum Mutat. dicembre 2018;39(12):1875–84.

49. Cannaerts E, Kempers M, Maugeri A, Marcelis C, Gardeitchik T, Richer J, et al. Novel pathogenic SMAD2 variants in five families with arterial aneurysm and dissection: further delineation of the phenotype. J Med Genet. aprile 2019;56(4):220–7.

50. Micha D, Guo DC, Hilhorst-Hofstee Y, van Kooten F, Atmaja D, Overwater E, et al. SMAD2 Mutations Are Associated with Arterial Aneurysms and Dissections. Hum Mutat. dicembre 2015;36(12):1145–9.

51. Van Gucht I, Meester JAN, Bento JR, Bastiaansen M, Bastianen J, Luyckx I, et al. A human importin-β-related disorder: Syndromic thoracic aortic aneurysm caused by bi-allelic loss-of-function variants in IPO8. Am J Hum Genet. 3 giugno 2021;108(6):1115–25.

52. Salmasi MY, Alwis S, Cyclewala S, Jarral OA, Mohamed H, Mozalbat D, et al. The genetic basis of thoracic aortic disease: The future of aneurysm classification? Hellenic Journal of Cardiology. gennaio 2023;69:41–50.

53. Goudie DR, D'Alessandro M, Merriman B, Lee H, Szeverényi I, Avery S, et al. Multiple self-healing squamous epithelioma is caused by a disease-specific spectrum of mutations in TGFBR1. Nat Genet. 27 febbraio 2011;43(4):365–9.

54. Loeys BL, Dietz HC. Loeys-Dietz Syndrome. In: Adam MP, Feldman J, Mirzaa GM, Pagon RA, Wallace SE, Amemiya A, curatori. GeneReviews® [Internet]. Seattle (WA): University of Washington, Seattle; 1993 [citato 3 giugno 2025]. Disponibile su: http://www.ncbi.nlm.nih.gov/books/NBK1133/

55. Camerota L, Ritelli M, Wischmeijer A, Majore S, Cinquina V, Fortugno P, et al. Genotypic Categorization of Loeys-Dietz Syndrome Based on 24 Novel Families and Literature Data. Genes (Basel). 28 settembre 2019;10(10):764.

56. Macias MJ, Martin-Malpartida P, Massagué J. Structural determinants of SMAD function in TGF-β signaling. Trends Biochem Sci. giugno 2015;40(6):296–308.

57. Hostetler EM, Regalado ES, Guo DC, Hanna N, Arnaud P, Muiño-Mosquera L, et al. SMAD3 pathogenic variants: risk for thoracic aortic disease and associated complications from the Montalcino Aortic Consortium. J Med Genet. aprile 2019;56(4):252–60.

58. Chesneau B, Edouard T, Dulac Y, Colineaux H, Langeois M, Hanna N, et al. Clinical and genetic data of 22 new patients with SMAD3 pathogenic variants and review of the literature. Mol Genet Genomic Med. maggio 2020;8(5):e1132.

59. de Wagenaar NP, van den Bersselaar LM, Odijk HJHM, Stefens SJM, Reinhardt DP, Roos-Hesselink JW, et al. Functional analysis of cell lines derived from SMAD3-related Loeys-Dietz syndrome patients provides insights into genotype-phenotype relation. Hum Mol Genet. 5 giugno 2024;33(12):1090–104.

60. Demolder A, Bianco L, Caruana M, Cervi E, Evangelista A, Jondeau G, et al. Arrhythmia and impaired myocardial function in heritable thoracic aortic disease: An international retrospective cohort study. Eur J Med Genet. giugno 2022;65(6):104503.

61. Backer JD, Braverman AC. Heart failure and sudden cardiac death in heritable thoracic aortic disease caused by pathogenic variants in the SMAD3 gene. Mol Genet Genomic Med. 1 maggio 2018;6(4):648–52.

62. Kay RT, Gouda P, Welsh RC. Cardiovascular pathology, inheritance and

prognosis in a familial cohort of Loeys-Dietz type III. Int J Cardiol. 1 luglio 2024;406:131984.

63. Li FF, Zhou J, Zhao DD, Yan P, Li X, Han Y, et al. Characterization of SMAD3 Gene Variants for Possible Roles in Ventricular Septal Defects and Other Congenital Heart Diseases. PLoS One. 2015;10(6):e0131542.

64. Solomonica A, Bagur R, Choudhury T, Lavi S. Familial Spontaneous Coronary Artery Dissection and the SMAD-3 Mutation. Am J Cardiol. 15 luglio 2019;124(2):313–5.

65. Faggion Vinholo T, Zafar MA, Ziganshin BA, Elefteriades JA. Nonsyndromic Thoracic Aortic Aneurysms and Dissections-Is Screening Possible? Semin Thorac Cardiovasc Surg. Winter 2019;31(4):628–34.

66. Rohde S, Zafar MA, Ziganshin BA, Elefteriades JA. Thoracic aortic aneurysm gene dictionary. Asian Cardiovasc Thorac Ann. settembre 2021;29(7):682–96.

67. Erbel R, Aboyans V, Boileau C, Bossone E, Di Bartolomeo R, Eggebrecht H, et al. [2014 ESC Guidelines on the diagnosis and treatment of aortic diseases]. Kardiol Pol. 2014;72(12):1169–252.

68. Toumpoulis IK, Oxford JT, Cowan DB, Anagnostopoulos CE, Rokkas CK, Chamogeorgakis TP, et al. Differential expression of collagen type V and XI alpha-1 in human ascending thoracic aortic aneurysms. Ann Thorac Surg. agosto 2009;88(2):506–13.

69. Jones JA, Spinale FG, Ikonomidis JS. Transforming growth factor-beta signaling in thoracic aortic aneurysm development: a paradox in pathogenesis. J Vasc Res. 2009;46(2):119–37.

70. Nagasawa A, Yoshimura K, Suzuki R, Mikamo A, Yamashita O, Ikeda Y, et al. Important role of the angiotensin II pathway in producing matrix metalloproteinase-9 in human thoracic aortic aneurysms. J Surg Res. luglio 2013;183(1):472–7.

71. Gomez D, Al Haj Zen A, Borges LF, Philippe M, Gutierrez PS, Jondeau G, et al. Syndromic and non-syndromic aneurysms of the human ascending aorta share activation of the Smad2 pathway. J Pathol. maggio 2009;218(1):131–42.

72. Harris SL, Lindsay ME. Role of Clinical Genetic Testing in the Management of Aortopathies. Curr Cardiol Rep. 21 gennaio 2021;23(2):10.

73. Beighton P, De Paepe A, Steinmann B, Tsipouras P, Wenstrup RJ. Ehlers-Danlos syndromes: revised nosology, Villefranche, 1997. Ehlers-Danlos National Foundation (USA) and Ehlers-Danlos Support Group (UK). Am J Med Genet. 28 aprile 1998;77(1):31–7.

74. Pepin M, Schwarze U, Superti-Furga A, Byers PH. Clinical and genetic features of Ehlers-Danlos syndrome type IV, the vascular type. N Engl J Med. 9 marzo 2000;342(10):673–80.

75. Pope FM, Narcisi P, Nicholls AC, Germaine D, Pals G, Richards AJ.

COL3A1 mutations cause variable clinical phenotypes including acrogeria and vascular rupture. Br J Dermatol. agosto 1996;135(2):163–81.

76. Siu SC, Silversides CK. Bicuspid aortic valve disease. J Am Coll Cardiol. 22 giugno 2010;55(25):2789–800.

77. El-Hamamsy I, Yacoub MH. A measured approach to managing the aortic root in patients with bicuspid aortic valve disease. Curr Cardiol Rep. marzo 2009;11(2):94–100.

78. McKellar SH, Tester DJ, Yagubyan M, Majumdar R, Ackerman MJ, Sundt TM. Novel NOTCH1 mutations in patients with bicuspid aortic valve disease and thoracic aortic aneurysms. J Thorac Cardiovasc Surg. agosto 2007;134(2):290–6.

79. Cripe L, Andelfinger G, Martin LJ, Shooner K, Benson DW. Bicuspid aortic valve is heritable. J Am Coll Cardiol. 7 luglio 2004;44(1):138–43.

80. Bravo-Jaimes K, Prakash SK. Genetics in bicuspid aortic valve disease: Where are we? Prog Cardiovasc Dis. 2020;63(4):398–406.

81. Milewicz DM, Guo DC, Tran-Fadulu V, Lafont AL, Papke CL, Inamoto S, et al. Genetic basis of thoracic aortic aneurysms and dissections: focus on smooth muscle cell contractile dysfunction. Annu Rev Genomics Hum Genet. 2008;9:283–302.

82. Fisher SA. Vascular smooth muscle phenotypic diversity and function. Physiol Genomics. 15 novembre 2010;42A(3):169–87.

83. Kwartler CS, Gong L, Chen J, Wang S, Kulmacz R, Duan XY, et al. Variants of Unknown Significance in Genes Associated with Heritable Thoracic Aortic Disease Can Be Low Penetrant «Risk Variants». Am J Hum Genet. 5 luglio 2018;103(1):138–43.

84. Guo DC, Hostetler EM, Fan Y, Kulmacz RJ, Zhang D, GenTAC Investigators, et al. Heritable Thoracic Aortic Disease Genes in Sporadic Aortic Dissection. J Am Coll Cardiol. 28 novembre 2017;70(21):2728–30.

85. Richards S, Aziz N, Bale S, Bick D, Das S, Gastier-Foster J, et al. Standards and guidelines for the interpretation of sequence variants: a joint consensus recommendation of the American College of Medical Genetics and Genomics and the Association for Molecular Pathology. Genet Med. maggio 2015;17(5):405–24.

86. Martín C, Evangelista A, Serrano-Fiz S, Villar S, Ospina V, Martínez D, et al. Aortic Complications in Marfan Syndrome: Should We Anticipate Preventive Aortic Root Surgery? Ann Thorac Surg. giugno 2020;109(6):1850–7.

87. Guo D chuan, Regalado E, Casteel DE, Santos-Cortez RL, Gong L, Kim JJ, et al. Recurrent gain-of-function mutation in PRKG1 causes thoracic aortic aneurysms and acute aortic dissections. Am J Hum Genet. 8 agosto 2013;93(2):398–404.

88. Best Practices Workflows – GATK [Internet]. [citato 20 agosto 2024]. Disponibile su: https://gatk.broadinstitute.org/hc/en-

us/sections/360007226651-Best-Practices-Workflows

89. Li H, Durbin R. Fast and accurate short read alignment with Burrows-Wheeler transform. Bioinformatics. 15 luglio 2009;25(14):1754–60.

90. Geraldine van der Auwera, Brian D. O'Connor. Genomics in the Cloud: Using Docker, GATK, and WDL in Terra. O'Reilly Media, Incorporated, 2020;

91. McLaren W, Gil L, Hunt SE, Riat HS, Ritchie GRS, Thormann A, et al. The Ensembl Variant Effect Predictor. Genome Biol. 6 giugno 2016;17(1):122.

92. Sulkava M, Raitoharju E, Mennander A, Levula M, Seppälä I, Lyytikäinen LP, et al. Differentially expressed genes and canonical pathways in the ascending thoracic aortic aneurysm – The Tampere Vascular Study. Sci Rep. 21 settembre 2017;7(1):12127.

93. Huckaby LV, Leshnower BG. Sex and Gender Differences in Aortic Disease. 6 luglio 2023 [citato 2 settembre 2025]; Disponibile su: https://www.uscjournal.com/articles/sex-and-gender-differences-aortic-disease?language_content_entity=en

94. Coady MA, Davies RR, Roberts M, Goldstein LJ, Rogalski MJ, Rizzo JA, et al. Familial Patterns of Thoracic Aortic Aneurysms. Arch Surg. 1 aprile 1999;134(4):361–7.

95. Patel ND, Crawford T, Magruder JT, Alejo DE, Hibino N, Black J, et al. Cardiovascular operations for Loeys-Dietz syndrome: Intermediate-term results. J Thorac Cardiovasc Surg. febbraio 2017;153(2):406–12.

96. Cury M, Zeidan F, Lobato AC. Aortic Disease in the Young: Genetic Aneurysm Syndromes, Connective Tissue Disorders, and Familial Aortic Aneurysms and Dissections. Int J Vasc Med. 2013;2013:267215.

97. Fusco C, Morlino S, Micale L, Ferraris A, Grammatico P, Castori M. Characterization of Two Novel Intronic Variants Affecting Splicing in FBN1-Related Disorders. Genes (Basel). 10 giugno 2019;10(6):442.

98. Takeda N, Inuzuka R, Maemura S, Morita H, Nawata K, Fujita D, et al. Impact of Pathogenic FBN1 Variant Types on the Progression of Aortic Disease in Patients With Marfan Syndrome. Circ Genom Precis Med. giugno 2018;11(6):e002058.

99. Arnaud P, Milleron O, Hanna N, Ropers J, Ould Ouali N, Affoune A, et al. Genotype-phenotype correlations in Marfan syndrome patients with FBN1 mutations: a cohort study on 1575 patients. Eur Heart J. 1 ottobre 2021;42(Supplement_1):ehab724.2015.

100. Franken R, Groenink M, de Waard V, Feenstra HMA, Scholte AJ, van den Berg MP, et al. Genotype impacts survival in Marfan syndrome. Eur Heart J. 14 novembre 2016;37(43):3285–90.

101. Franken R, Heesterbeek TJ, de Waard V, Zwinderman AH, Pals G, Mulder BJ, et al. Diagnosis and genetics of Marfan syndrome. Expert Opinion on Orphan Drugs. 1 ottobre 2014;2(10):1049–62.

102. Davis MR, Arner E, Duffy CRE, De Sousa PA, Dahlman I, Arner P, et al. Expression of FBN1 during adipogenesis: Relevance to the lipodystrophy phenotype in Marfan syndrome and related conditions. Mol Genet Metab. settembre 2016;119(1–2):174–85.

103. Summers KM, Nataatmadja M, Xu D, West MJ, McGill JJ, Whight C, et al. Histopathology and fibrillin-1 distribution in severe early onset Marfan syndrome. Am J Med Genet A. 15 novembre 2005;139(1):2–8.

104. Stengl R, Bors A, Ágg B, Pólos M, Matyas G, Molnár MJ, et al. Optimising the mutation screening strategy in Marfan syndrome and identifying genotypes with more severe aortic involvement. Orphanet J Rare Dis. 15 ottobre 2020;15(1):290.

105. Meier N, Bruder E, Miny P, Tercanli S, Filges I. Expanding the spectrum of SMAD3-related phenotypes to agnathia-otocephaly. Mol Genet Genomic Med. aprile 2020;8(4):e1178.

106. Richer J, Velchev JD, Goobie S, Boswell-Patterson CA, van de Laar IMBH, Verhagen JMA, et al. Sexual dimorphism in SMAD3 pathogenic variant-harbouring individuals. J Med Genet. 26 febbraio 2025;62(3):199–205.

107. Dekker S, Thijssen CGE, Linde D vd, vd Laar IMBH, Saris JJ, van Es ACGM, et al. Neurovascular abnormalities in patients with Loeys-Dietz syndrome type III. European Journal of Medical Genetics. 1 febbraio 2022;65(2):104424.

108. Laterza D, Ritelli M, Zini A, Colombi M, Dell'Acqua ML, Vandelli L, et al. Novel pathogenic *TGFBR1* and *SMAD3* variants identified after cerebrovascular events in adult patients with Loeys-dietz syndrome. European Journal of Medical Genetics. 1 ottobre 2019;62(10):103727.

109. Garcia-Bermúdez M, Moustafa AH, Barrós-Membrilla A, Tizón-Marcos H. Repeated Loss of Consciousness in a Young Woman: A Suspicious *SMAD3* Mutation Underlying Spontaneous Coronary Artery Dissection. Canadian Journal of Cardiology. 1 febbraio 2017;33(2):292.e1-292.e3.

110. Asokan KL, Landes JR, Renders W, Mosquera LM, Backer JD, Jantzen DW, et al. Mitral Annular Disjunction in Heritable Thoracic Aortic Disease: Insights From the Montalcino Aortic Consortium.

111. Calderon-Martinez E, Velasco WV, Guo D, Hostetler EH, Xun Z, Stephens S, et al. Differences in Arterial Events in Vascular Ehlers-Danlos, Loeys-Dietz, and Marfan Syndrome. J Am Coll Cardiol. 24 giugno 2025;85(24):2355–67.

112. Yagyu T, Noguchi T, Asano Y, Ida K, Ogata S, Nishimura K, et al. Association Between Genetic Diagnosis and Clinical Outcomes in Patients With Heritable Thoracic Aortic Disease. J Am Heart Assoc. 18 aprile 2023;12(8):e028625.

113. Mühlstädt K, De Backer J, von Kodolitsch Y, Kutsche K, Muiño Mosquera L, Brickwedel J, et al. Case-matched Comparison of Cardiovascular Outcome in Loeys-Dietz Syndrome versus Marfan Syndrome. J Clin Med. 29 novembre 2019;8(12):2079.